π-π Interactions and bandwidths in "molecular metals". A chemical, structural, photoelectron spectroscopic, and Hartree-Fock-Slater study of monomeric and cofacially joined dimeric...

ARTICLE *in* JOURNAL OF THE AMERICAN CHEMICAL SOCIETY · APRIL 1984

Impact Factor: 12.11 · DOI: 10.1021/ja00337a018

π-π Interactions and Bandwidths in "Molecular Metals". A Chemical, Structural, Photoelectron Spectroscopic, and Hartree-Fock-Slater Study of Monomeric and Cofacially Joined Dimeric Silicon Phthalocyanines

E. Ciliberto,[1a] K. A. Doris,[1b] W. J. Pietro,[1b] G. M. Reisner,[1c] D. E. Ellis,*[1b] I. Fragalà,*[1a] F. H. Herbstein,*[1c] M. A. Ratner,*[1b] and T. J. Marks*[1b]

Contribution from the Department of Chemistry and the Materials Research Center, Northwestern University, Evanston, Illinois 60201, Dipartimento di Chimica, Universita di Catania, 95125 Catania, Italy, and the Department of Chemistry, Technion-Israel Institute of Technology, Haifa, 32000 Israel. *Received May 3, 1984*

Abstract: This contribution describes an integrated chemical, physical, and quantum chemical approach to understanding π-π interactions and tight-binding bandwidths in low-dimensional metallomacrocyclic "metals" via the properties of monomeric and dimeric stack fragments. Thus, electronic structure in the cofacially arrayed phthalocyaninato (Pc) polymer $[Si(Pc)O]_n$ has been explored through the complexes $Si(Pc)(OR)_2$ and $ROSi(Pc)OSi(Pc)OR$ ($R = Si[C(CH_3)_3](CH_3)_2$). Improved synthetic and purification procedures are described. Vibrational spectroscopy is employed to assign ROSi and Si(Pc)OSi(Pc) modes, and the results are correlated with data on $[Si(Pc)O]_n$. The cofacial dimer crystallizes from chloroform in the orthorhombic space group *Pbcn* (No. 60) with four molecules in a unit cell of dimensions $a = 21.670$ (8), $b = 13.724$ (5), and $c = 23.031$ (9) Å. Least-squares refinement led to a value for the conventional R index (on F) of 0.127 for 1975 independent reflections having $5° \leq 2\sigma_{MoK\bar{\alpha}} \leq 40°$ and $F_o \geq 3\sigma(F_o)$. The molecular structure consists of a cofacial (Pc)Si-O-Si(Pc) core of C_2 symmetry, having virtually planar phthalocyanine rings, an Si-Si distance (interplanar spacing) of 3.32 (1) Å, ∠Si-O-Si = 179 (1)°, and a ring-ring staggering angle of 36.6°. The $Si[C(CH_3)_3](CH_3)_2$ capping groups are disordered. Electronic structure in the (phthalocyaninato)silicon monomer and dimer has been studied with first principles discrete variational local exchange (DV-Xα) techniques. These results are combined with transition-state calculations to interpret optical and high resolution He I and He II photoelectron spectroscopic data. While the conventional porphyrinic "four-orbital" model is supported for the low-energy optical transitions (excellent agreement between observed and calculated energies is noted), possible disagreements are noted at higher energies. Calculated (6.8 eV) and observed (6.46 eV) $Si(Pc)(OR)_2$ ionization potentials are in good agreement. The lowest energy PES feature in the dimer is split by 0.29 (3) eV. The splitting can be assigned to the cofacial HOMO-HOMO interaction and translates to a tight-binding bandwidth in the polymer of 0.58 (6) eV. This result is in favorable agreement with a DV-Xα derived bandwidth of 0.76 eV and a value of 0.60 (6) eV previously obtained from a Drude analysis on $\{[Si(Pc)O]I_{1.12}\}_n$. These results argue that the principal charge-transport pathway in the $[Si(Pc)O]_n$ polymer is via the Pc π systems and that polaronic band-narrowing effects are minimal.

An indispensable prerequisite for understanding the optical, magnetic, charge-transport, architectural, and thermodynamic characteristics of solids composed of arrays of conjugated organic/metal-organic molecular constituents[2] is the nature and magnitude of the interactions between neighboring π-electron systems. Experimental approaches to acquiring information such as expressed by the tight-binding bandwidth[2] have included in situ magnetic,[2,3] optical,[2,4] and thermoelectric power[2,5] measurements. Each approach has significant limitations (e.g., Coulomb correlations leading to pronounced susceptibility enhancements in the case of magnetic measurements),[3,5a,6] and, indeed, for a variety of materials, there is considerable disagreement between bandwidth parameters measured by different approaches. Theoretically, strategies for quantifying π-π interactions have included more rigorous calculations on hypothetical molecular dimers[7] or pragmatically less rigorous calculations (e.g., "crystal orbital") on arrays of molecules or of molecular fragments.[8]

Over the past several years, we have been carrying out a detailed study of a new class of low-dimensional molecular conductors in which conjugated metallomacrocyclic subunits such as phthalocyanines are rigorously constrained in a cofacial orientation by intervening covalent bonds (**1**).[9] Thus, stacking architecture is, for the first time in a molecular conductor, rigidly enforced and,

(1) (a) Università di Catania. (b) Northwestern University. (c) Technion Israel Institute of Technology.

(2) Comes, R.; Bernier, P.; Andre, J. J.; Rouxel, J. "Proceedings of the International Conference on Low-Dimensional Conductors and Superconductors"; Les Arcs-Bourg-Saint-Maurice Savoie: France, Dec 1982 (*J. Phys.* **1983** C3). (b) Miller, J. S., Ed. "Extended Linear Chain Compounds"; Vols. 1, 2, and 3, Plenum Press: New York, 1982; Vols. 1-3. (c) Epstein, A. J.; Conwell, E. M., Eds., "Proceedings of the International Conference on Low-Dimensional Conductors"; Boulder, CO, Aug 1981 (*Mol. Cryst. Liq. Cryst.* **1981-1982**, Parts A-F. (d) Alcâcer, L., Ed. "The Physics and Chemistry of Low-Dimensional Solids"; D. Reidel: Dordrecht, 1980. (e) Devreese, J. T., Evrard, B. P., van Doren, V. E., Eds. "Highly Conducting One-Dimensional Solids"; Plenum Press: New York, 1979. (f) Hatfield, W. E., Ed., "Molecular Metals"; Plenum Press: New York, 1979.

(3) (a) Shiba, H. *Phys. Rev. B: Solid State* **1972**, *6*, 930-938. Torrance, J. B.; Tomkiew, Y.; Silverman, B. D. *Phys. Rev. B: Solid State* **1977**, *15*, 4738-4749.

(4) (a) Tanner, D. B. in ref 2b, Vol. 2, pp 205-258. (b) Madison, M. R.; Coleman, L. B.; Somoano, R. B. *Solid State Commun.* **1981**, *40*, 979-982. (c) Weinstein, B. A.; Slade, M. L.; Epstein, A. J.; Miller, J. S. *Solid State Commun.* **1981**, *37*, 643-646 and references therein. (d) Torrance, J. B.; Scott, B. A.; Welber, B.; Kaufman, F. B.; Seiden, P. E. *Phys. Rev. B: Condens. Matter* **1979**, *19*, 730-741. (e) Delhaes, P.; Coulon, C.; Amiell, J.; Flandrois, S.; Toreilles, E.; Fabre, J. M.; Giral, L. *Mol. Cryst. Liq. Cryst.* **1979**, *50*, 43-58. (f) Jacobsen, C. S.; Mortensen, K.; Andersen, J. R.; Bechgaard, K. *Phys. Rev. B: Condens. Matter* **1978**, *18*, 905-921. (g) Somoano, R. B.; Yen, S. P. S.; Hadek, V.; Khanna, S. K.; Novotny, M.; Datta, T.; Hermann, A. M.; Woollam, J. A. *Phys. Rev. B: Condens. Matter* **1978**, *17*, 2853-2857.

(5) Mortensen, K.; Conwell, E. M.; Fabre, J. M. *Phys. Rev. B: Condens. Matter* **1983**, *28*, 5856-5862. (b) Mortensen, K. *Solid State Commun.* **1982**, *44*, 643-647. (c) Chaikin, P. M.; Greene, R. L.; Etemad, S.; Engler, E. *Phys. Rev. B: Solid State* **1976**, *13*, 1627-1632.

(6) See, for example: (a) Delhaes, P. *Mol. Cryst. Liq. Cryst.* **1983**, *96*, 229-262. (b) Coulon, C.; Delhaes, P.; Flandrois, S.; Lagnier, R.; Bonjour, E.; Fabre, J. M. *J. Phys.* **1982**, *43*, 1059-1066.

(7) (a) Grant, P. M. *Phys. Rev. B: Condens. Matter.* **1983**, *27*, 3934-3947. (b) Grant, P. M. *Phys. Rev. B: Condens. Matter* **1982**, *26*, 6888-6895 and references therein. (c) Herman, F. *Phys. Scr.* **1977**; *16*, 303-306. (d) Herman, F.; Salahub, D. R.; Messmer, R. P. *Phys. Rev. Solid State* **1977**, *16*, 2453-2465.

(8) (a) Wangbo, M.-Y. in ref 2b, Vol. 2, pp 127-158. (b) Honeybourne, C. L. *J. Chem. Soc., Chem. Commun.* **1982**, 744-745. (c) Böhm, M. C. *Solid State Commun.* **1983**, *45*, 117-120 and references therein. (d) Whangbo, M.-H.; Stewart, K. R. *Isr. J. Chem.* **1983**, *23*, 133-138. (e) Alvarez, S.; Canadell, E. *Solid State Commun.* **1984**, *50*, 141-144. (f) Canadell, E.; Alvarez, S. *Inorg. Chem.* **1984**, *23*, 573-579. (g) Böhm, M. C. *Chem. Phys.* **1984**, *86*, 17-30.

(9) (a) Marks, T. J.; Kalina, D. W. in ref 2b, Vol. 1, pp 197-331. (b) Hanack, M. *Chimia* **1983**, *37*, 238-245 and references therein.

0002-7863/84/1506-7748$01.50/0

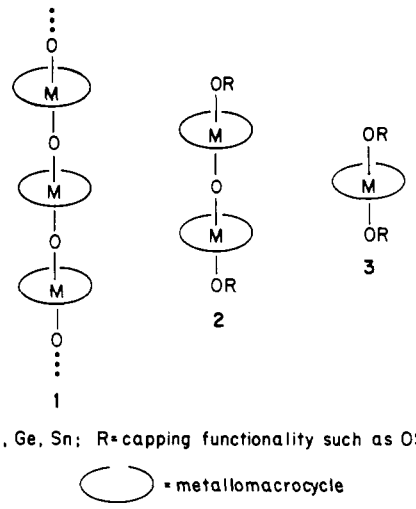

moreover, variable as the covalent radius of M is altered. For the phthalocyaninato system $[M(Pc)O]_n$[10] detailed studies of crystal structure, magnetism, optical properties, charge transport, etc. have been possible for a wide range of inorganic and organic "dopants" (electron acceptors and donors).

An equally fascinating consequence of the connectivity of the cofacially joined metallomacrocyclic low-dimensional conductors is the subject of this contribution. The dimers of the previous aforementioned theoretical studies need no longer be purely hypothetical constructs but are isolable molecular entities (**2**) that can be subjected to correlated physicochemical and theoretical investigation. In particular, it can be demonstrated by perturbation theoretical arguments[7c] that the magnitude of the π–π HOMO–HOMO interaction in a M(Pc)OM(Pc) cofacial dimer can be straightforwardly extrapolated to the tight-binding bandwidth in the corresponding $[M(Pc)O]_n$ polymer (Figure 1). Moreover, the HOMO–HOMO interaction is the type of "through-space" MO–MO interaction that can be quantitatively assessed by gas-phase photoelectron spectroscopy (PES).[11] In the present contribution, we report on the properties of the M = Si monomer (**3a**) and dimer (**2a**) where R = $Si[C(CH_3)_3](CH_3)_2$. This discussion includes improved synthetic[12] procedures for **2a** and **3a**, the determination of the molecular structure of **2a** by single-crystal diffraction methods (which complements earlier structural information obtained on $[Si(Pc)O]_n$ by analysis of powder data[10b]), an analysis of the vibrational spectra relevant to spectral assignments, to guiding syntheses of other cofacial metallomacrocyclic oligomers, and, ultimately, to studies of electron–phonon coupling in the corresponding polymers, an analysis of the optical spectra as they relate to ring–ring interactions and electronic structure, a presentation of He I and He II spectra,[13]

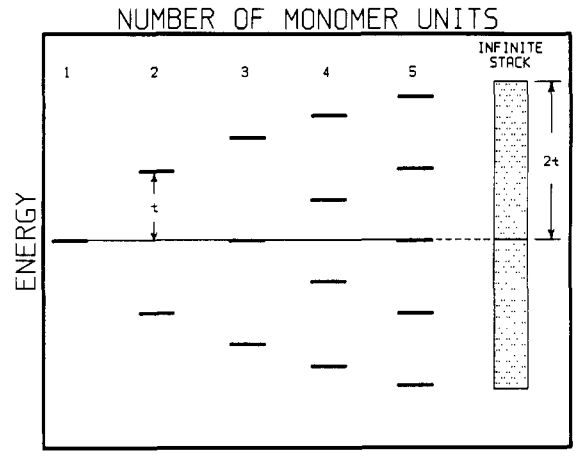

Figure 1. Scheme illustrating the energetics of arraying increasing numbers of subunit highest occupied molecular orbitals, resulting ultimately in band formation. The parameter t is the tight-binding transfer integral, analogus to the Hückel β integral.

acquired, processed, and analyzed by modern digital techniques, and finally, an integrated study of the electronic structures of **2a** and **3b** by the first principles discrete variational method local exchange (DV-Xα) technique.[14,15] We have recently shown that this formalism accurately describes the electronic structure of arenes[16] as well as "through-space" (π–π) and "through-bond" (π–σ–π) interactions in [2.2]paracyclophane.[17]

Experimental Section

Elemental anaylses were performed by Microtech Laboratories (Skokie, IL), or Galbraith Laboratories (Knoxville, TN). Quinoline was vacuum distilled from BaO and pyridine distilled under N_2 from BaO. Methanol was distilled from magnesium under N_2. Silicon tetrachloride (Alfa) was distilled under N_2 immediately prior to use. Practical grade *o*-phthalonitrile (Eastman) was dried for at least 24 h under vacuum (10^{-3} torr). Ammonia (Matheson, anhydrous) and *tert*-butyldimethylchlorosilane (Petrarch) were used without further purification. In general, any reaction requiring a nitrogen atmosphere was carried out in glassware that was dried by evacuation (10^{-3} torr) and flaming, and all solids (except *tert*-butyldimethylchlorosilane) was dried under vacuum (10^{-3} torr) in such glassware overnight. Sublimations were carried out in a Lindberg Hevi-Duty type No. 54031A tube oven. The temperature was raised by intervals of about 5 °C approximately every 3 h, and the tube was moved slightly toward the outside of the oven so that material would form successive temperature bands. Temperature ranges reported produced bands of the same (pure) substance.

Synthesis of 1,3-Diiminoisoindoline. 1,3-Diiminoisoindoline was synthesized from *o*-phthalonitrile by a modification of the literature procedure.[10b,18] The reaction solution was refluxed for 5 h, and then NH_3 addition and heating were discontinued, but mechanical stirring under N_2 atmosphere was continued for 75 min, or until cool. The light green slurry was filtered at room temperature, yielding a light green powder, mp 185–190 °C. This product was stirred in ether and filtered twice, sharpening the melting point to 193–195 °C. The dark green reaction solution and the other washes were cooled in dry ice/acetone baths until no more solid precipitated. This product was filtered off and purified as above. The total yield of light green product was 52% (based on *o*-phthalonitrile).

Synthesis of Si(Pc)Cl$_2$. (Phthalocyaninato)silicon dichloride was prepared by the literature method,[10b] with yields ranging from 60% to 75%.

(10) (a) Diel, B. N.; Inabe, T.; Lyding, J. W.; Schoch, K. F., Jr.; Kannewurf, C. R.; Marks, T. J. *J. Am. Chem. Soc.* **1983**, *105*, 1551–1567. (b) Dirk, C. W.; Inabe, T.; Schoch, K. F., Jr.; Marks, T. J. *J. Am. Chem. Soc.* **1983**, *105*, 1539–1550. (c) Dirk, C. W.; Inabe, C. W.; Lyding, J. W.; Schoch, K. F., Jr.; Kannewurf, C. R.; Marks, T. J. *J. Polym. Sci., Polym. Symp.* **1983**, *70*, 1–29. (d) Inabe, T.; Lyding, J. W.; Moguel, M. K.; Marks, T. J. *J. Phys.* **1983**, *C3*, 625–631. (e) Inabe, T.; Kannewurf, C. R.; Lyding, J. W.; Moguel, M. K.; Marks, T. J. *Mol. Cryst. Liq. Cryst.* **1983**, *93*, 355–367. (f) Dirk, C. W.; Schoch, K. F., Jr.; Marks, T. J. *Polym. Sci. Technol.* **1981**, *15*, 209–226. (g) Dirk, C. W.; Mintz, E. A.; Schoch, K. F., Jr.; Marks, T. J. *J. Macromol. Sci. Chem.* **1981**, *A16*, 275–298. (h) Marks, T. J.; Schoch, K. F., Jr.; Kundalkar, B. R. *Synth. Met.* **1980**, *1*, 337–347. (i) Schoch, K. F., Jr.; Kundalkar, B. R.; Marks, T. J. *J. Am. Chem. Soc.* **1979**, *101*, 7071–7073.

(11) (a) Heilbronner, E.; Yang, Z.-Z. *Top. Curr. Chem.* **1983**, *115*, 1–55. (b) Paddon-Row, M. N. *Acc. Chem. Res.* **1982**, *15*, 245–251. (c) Gleiter, R. *Angew. Chem. Int. Ed. Engl.* **1974**, *13*, 696–701. (d) Hoffmann, R.; Imamura, A.; Hehre, W. J. *J. Am. Chem. Soc.* **1968**, *90*, 1499–1509. (e) Hoffmann, R. *Acc. Chem. Res.* **1971**, *4*, 1–9.

(12) For previous synthetic work, producing what appear to be somewhat less pure materials, see: Mezza, T. M.; Armstrong, N. R.; Ritter, G. W. II; Iafalice, J. P.; Kenney, M. E. *J. Electroanal. Chem.* **1982**, *137*, 227–237.

(13) For an early, lower resolution study at a single photon energy on related compounds, but not directed at the electronic structures of low-dimensional conductors, see: Hush, N. S.; Cheung, A. S. *Chem. Phys. Lett.* **1977**, *47*, 1–4.

(14) (a) Baerends, E. J.; Ellis, D. E.; Ros, P. *Chem. Phys.* **1973**, *2*, 41–51. (b) Berkovitch-Yelln, Z.; Ellis, D. E.; Ratner, M. A. *Chem. Phys.* **1981**, *62*, 21–35. (c) Delley, B.; Ellis, D. E. *J. Chem. Phys.* **1982**, *76*, 1949–1960. (d) Rosen, A.; Ellis, D. E.; Adachi, H.; Averill, F. W. *J. Chem. Phys.* **1975**, *65*, 3269–3634. (e) Ondrechen, M. J.; Ratner, M. A.; Ellis, D. E. *J. Am. Chem. Soc.* **1981**, *103*, 1656–1659.

(15) Pietro, W. J.; Ellis, D. E.; Marks, T. J.; Ratner, M. A. *Mol.Cryst. Liq. Cryst.* **1984**, *105*, 273–287.

(16) Doris, K. A.; Ratner, M. A.; Ellis, D. E.; Marks, T. J. *J. Phys. Chem.* **1984**, *88*, 3157–3159.

(17) Doris, K. A.; Ellis, D. E.; Ratner, M. A.; Marks, T. J. *J. Am. Chem. Soc.* **1984**, *106*, 2491–2497.

(18) Lowery, M. K.; Starshak, A. J.; Esposito, J. N.; Krueger, P. C.; Kenney, M. E. *Inorg. Chem.* **1965**, *4*, 128.

Synthesis of $Si(Pc)(OH)_2$. (Phthalocyaninato)silicon dihydroxide was prepared by the method of Davison and Wynne[19] by hydrolysis of finely ground $Si(Pc)Cl_2$ with pyridine and aqueous NaOH. This procedure was modified by repeating the hydrolysis two more times, with slightly more pyridine and less aqueous NaOH each time. The product was ground carefully before each hydrolysis and was filtered from the solution immediately after being cooled to avoid decomposition.

Anal. Calcd for $C_{32}H_{18}N_8O_2Si$: C, 66.89; H, 3.16; N, 19.50; Cl, 0.00. Found for thrice-hydrolyzed product: C, 66.89; H, 3.34; N, 19.60; Cl, 0.12.

The infrared spectrum (Nujol mull) corresponded to that previously reported.[10b]

Synthesis of $Si(Pc)\{OSi(CH_3)_2[C(CH_3)_3]\}_2$ (3a). Dicapped monomer was synthesized by using a modification of the method of Mezza et al.[12] Distilled pyridine (100 mL) was added to vacuum-dried $Si(Pc)(OH)_2$ (2.91 g, 5.064 mmol) under an N_2 flush. Meanwhile, 250 mL of distilled pyridine was added to an eightfold excess of *tert*-butyldimethylchlorosilane (12.12 g, 80.42 mmol) under N_2. The two solutions were combined under N_2 flush, and the mixture was refluxed for 92 h. The solid product (3.78 g) was then filtered from the solution and washed with pentane (50 mL) and 1:1 methanol/water (200 mL). These washes contain trace amounts of the more soluble dimer **2a** as judged by visible spectrophotometry. No further purification of the resulting monomer was necessary. The yield was 3.62 g (89%). The dicapped monomer begins to sublime at 240 °C (10^{-3} torr).

Anal. Calcd for $C_{44}H_{46}N_8O_2Si_3$: C, 65.80; H, 5.77; N, 13.95; Si, 10.49. Found: C, 65.78; H, 5.87; N, 13.78; Si, 10.68.

Infrared spectrum (Nujol mull): 1610 m, 1595 vw, 1518 s, 1430 s, 1404 w, 1367 m, 1350 m, 1343 vs, 1290 s, 1239 s, 1166 m, 1120 vs, 1079 vs, 1072 w, 1050 vs (br), 1003 m, 975 w, 950 w, 940 w, 910 s, 869 m, 832 vs, 810 vw, 770 s, 758 s, 733 vs, 698 w, 674 w, 645 w, 630 w, 575 m, 562 m, 530 s, 424 m cm^{-1}.

Synthesis of $[C(CH_3)_3](CH_3)_2SiO[Si(Pc)O]_2Si(CH_3)_2[C(CH)_3]$ (2a). Dicapped dimer was prepared by using a modification of the method of Mezza et al.[12] (Phthalocyaninato)silicon dichloride (5.5615 g, 9.094 mmol) and (phthalocyaninato)silicon dihydroxide (4.9500 g, 8.614 mmol) were vacuum desiccated overnight and then refluxed for 2.5 h in dry quinoline (500 mL) under an N_2 atmosphere. This product was filtered off, washed with 300 mL of 1:1 acetone/water, vacuum dried, and finely ground. This compound is formulated as HOSi(Pc)OSi(Pc)Cl (**4**) on the basis of infrared spectroscopy (vide infra). It was hydrolyzed in a mixture of 700 mL of pyridine, 100 mL of distilled water, and 30.00 g of NaOH by refluxing for 27 h. The resulting solid was then filtered off and washed with 1:1 acetone/water. After thorough vacuum desiccation, this solid, which is formulated as $HO[Si(Pc)O]_2H$ (**5**) on the basis of infrared spectroscopy (vide infra) (3.3407 g, 2.953 mmol assuming it is pure), was refluxed with $Si[C(CH_3)_3](CH_3)_2Cl$ (approximately 6.0 g, 40 mmol) in dry pyridine (500 mL) under an N_2 atmosphere for 13 h. The solvent was then removed under vacuum. Workup of the product was as described in the literature,[12] giving ca. 1.75 g of dicapped dimer (>90% pure by ^1H NMR), a 15% overall yield basd on $Si(Pc)(OH)_2$. The product is a bluish-purple powder, deep blue in organic solvents. Rectangular crystals for diffraction studies (the largest, 4 mm × 0.40 mm × 2.0 mm) were grown from an almost saturated chloroform solution by slow evaporation. Purification by vacuum sublimation (300–340 °C (10^{-3} torr)) produced very pure microcrystalline product, but in only a 5% yield.

Anal. Calcd for $C_{76}H_{62}N_{16}O_3Si_4$: C, 67.13; H, 4.60; N, 16.48; Si, 8.26. Found, single crystals: C, 67.80; H, 4.58; N, 16.53. Found, powder: C, 66.33; H, 4.70; N, 16.22; Si, 8.09.

Infrared spectrum (Nujol mull): 1614 m, 1596 vw, 1520 s, 1429 s, 1355, m 1338 s, 1290 s, 1250 m(br), 1167 s, 1122 s, 1080 vs, 1038 vs, 1004, w, 987 w, 978 w, 948 vw, 910 s, 872 vw, 867 w, 830 m, 804 w, 759 s, 730 vs, 645 w, 575 m, 530 m cm^{-1}.

Synthesis of $Si[C(CH_3)_3](CH_3)_2OH$. The general procedure of Sommer et al.[20] was employed for the hydrolysis of $Si[C(CH_3)_3](CH_3)_2Cl$ with slight modification. The hygroscopic chlorosilane (17.00 g, 0.113 mmol) was weighed out in a glovebag and then dissolved in 200 mL of diethyl ether. This solution was added dropwise with stirring over ca. 1 h (0 °C) to a mixture of 100 mL of H_2O, 25 mL of CH_3OH, and 7.0 g of KOH. The resulting milky white layers were next separated, and the aqueous layer was extracted with 3 × 150 mL of ether. The solvent was then distilled from the combined ether solutions at atmospheric pressure (under N_2). Distillation of the waxy white residue (predominantly $Si[C(CH_3)_3](CH_3)_2OH \cdot {}^1/_2H_2O$) melting at 80–90 °C (lit. mp 79 °C) bath temperature was next carried out. Between 95 and 130 °C, a solid fraction (the hemihydrate) was collected (gentle heating was applied to prevent clogging of the collection apparatus) and, at 140 °C, a colorless liquid (the anhydrous silanol, lit. bp 141 °C) distilled. The hemihydrate was partially converted to $Si[C(CH_3)_3](CH_3)_2OH$ by storage at reduced pressure in a vessel containing an adjacent chamber of P_2O_5. The anhydrous silanol was then drawn off by syringe. Both products were characterized by ^1H NMR and IR spectroscopy.

Infrared Spectroscopy. Infrared spectra were recorded on a Perkin-Elmer Model 283 or 599-B spectrophotometer. Polystyrene film was used as the reference for calibration. Samples were examined as Nujol mulls between KBr plates. Nujol on KBr plates was sometimes placed in the reference beam to clarify the region below 500 cm^{-1}.

Mass Spectroscopy. Mass spectral data on the silicon phthalocyanine monomer $Si(Pc)\{OSi(CH_3)_2[C(CH_3)_3]\}_2$ were recorded on a Hewlett-Packard 5985 GC/MS by Dr. Doris Hung, at 45-eV ionization energy, with 113 scans from 50 to 850 amu.

NMR Spectroscopy. Proton magnetic resonance spectra were recorded for all reasonably soluble products on a JEOL FX-90 or FX-270 Fourier-transform instrument. Spectra were referenced to the residual proton signal in the deuterated solvent in all cases. Appropriately long pulse delays (typically 2 s) were employed in cases where accurate integration was desired.

Optical Spectroscopy. All UV–visible spectra were taken on solutions by using a number of different solvents (see Results) in quartz cells of 1-cm path length. Optical spectra were measured on water-sensitive compounds, primarily the Si–Cl compounds, by using an airtight quartz cell fitted with a Kontes valve. All spectra were recorded on a Perkin-Elmer Model 330 spectrophotometer against the pure solvent as reference. A Perkin-Elmer Model 320 Data Station, interfaced to the 330, was used for data storage on a Verbatim floppy disk and for replotting of spectra.

Photoelectron Spectroscopy. He I and He II photoelectron spectra of the dicapped monomer and dimer were recorded on a Perkin-Elmer PS18 spectrometer modified for He II measurements by including a hollow cathode lamp producing a high photon flux at the He II wavelength (Helectros Development Co.).[21] The spectra were accumulated in the "multiple scan mode" with the aid of a MOSTEK computer directly interfaced to the spectrometer. The energy scales of each scan were locked to the reference value of the Ar $^2P_{3/2}$ and of He $1s^{-1}$ self-ionization lines. Deconvolution of the spectra was accomplished by fitting the spectral profiles with a series of asymmetrical Gaussian curves after subtraction of the background. The areas of bands thus evaluated can be affected by errors smaller than 5%.

X-ray Diffraction Study of $[C(CH_3)_3](CH_3)_2SiO[Si(Pc)O]_2Si(CH_3)_2[C(CH_3)_3]$ (2a).[22] The crystal used for data collection had an irregular shape (dimensions 0.1 × 0.1 × 0.2 mm) and was sealed in a Lindemann glass capillary to prevent possible decomposition. The density of the crystal was measured by flotation in a mixture of cyclohexane/tetrabromoethane. Cell dimensions and systematic absences were determined at 25 ± 1 °C by using a Philips PW1100 four-circle diffractometer with graphite-monochromated Mo Kα radiation and 1.15°-wide ω scans at a speed of 0.016 ω deg/s. The intensities of 1975 reflections with $F_o \gtrsim 3\sigma(F_o)$ were used in the structure analysis; absorption corrections were not applied, as μ(Mo Kα) = 1.10 cm^{-1}. The structure was solved by a combination of Patterson and direct methods. Calculations were carried out by using the SHELX-77 set of programs[23] on the IBM 370-168 computer at the Technion. Refinement was hampered by disorder of the $Si[C(CH_3)_3](CH_3)_2$ capping groups, and convergence was achieved at $R_F = 0.127$,[22] with anisotropic thermal parameters for ordered non-hydrogen atoms, and isotropic Debye–Waller factors for hydrogen atoms and the disordered atoms of the capping groups. The disorder was interpreted in terms of a major (occupancy 0.5) and two minor (occupancies each 0.25) orientations. All the non-hydrogen disordered atoms in the major orientation were located from successive Fourier maps, but not all the terminal carbon atoms of the *tert*-butyl groups of the caps could be located in the minor orientations. Details concerning the crystal, data collection, and data refinement are summarized in Table I.

Results

Synthesis Strategies for 2a and 3a. The preparative goal of this project was to prepare isolable –Si(Pc)– and –Si(Pc)OSi(Pc)–

(19) Davison, J. B.; Wynne, K. J. *Macromolecules* **1978**, *11*, 186–191.
(20) (a) Sommer, L. H.; Tyler, L. J. *J. Am. Chem. Soc.* **1954**, *76*, 1030–1033. (b) Sommer, L. H.; Evans, F. J. *J. Am. Chem. Soc.* **1954**, *76*, 1186–1187.
(21) Ciliberto, E.; Condorelli, G.; Fagan, P. J.; Manriquez, J. M.; Fragalà, I.; Marks, T. J. *J. Am. Chem. Soc.* **1981**, *103*, 4755–4759.
(22) See paragraph at end of paper regarding supplementary material.
(23) Sheldrick G. M. SHELX-77, a Program for Crystal Structure Determination; Univertisy of Cambridge: Cambridge, England, 1977.

Table I. Crystal Data and Intensity Measurement Conditions for $[C(CH_3)_3](CH_3)_2SiO[Si(Pc)O]_2Si(CH_3)_2[C(CH_3)_3]$ (**2a**)

a, Å	21.670 (8)
b, Å	13.724 (5)
c, Å	23.031 (9)
space group	*Pbcn* (No. 60)
vol., Å^3	6849.4
Z	4
mol formula	$Si_4O_3N_{16}C_{76}H_{62}$
mol wt	1358.9
D_m(g·cm^{-3})[a]	1.30
D_{calcd}	1.32
radiatn	Mo Kα
μ cm^{-1}	1.10
speed, ω°/s	0.016
slit width, °ω	1.15
background (total, s)	20
method	$\omega/2\theta$
θ limits, deg	$5 \leq 2\theta \leq 40°$
no. of reflctns for which $F_o > 3.0\sigma(F_o)$	1975
R_F	12.7%

[a] Measured by flotation in a mixture of cyclohexane/tetrabromoethane.

Scheme I

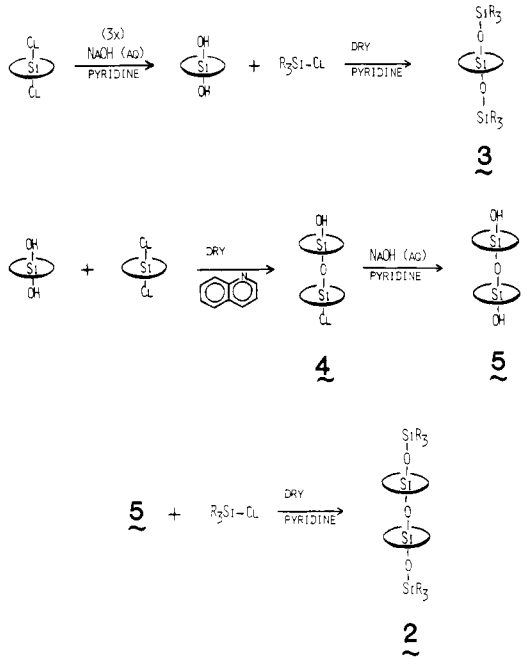

fragments in *high purity* for physicochemical investigation. Stability with respect to dehydration condensation (eq 1) is crucial

$$2\ \text{–Si(Pc)OH} \xrightarrow{H_2O} \text{–Si(Pc)–O–Si(Pc)–} \qquad (1)$$

for gas-phase PES studies, in view of the volatilization temperatures generally required for metallophthalocyanines[24] and related porphyrins.[25] Thus, the siloxy derivatization ("capping") approach outlined in Scheme I was employed for the syntheses of **2a** and **3a**. This methodology was originally developed by Kenney;[12,26] however, in our hands, several precautions/modifications were

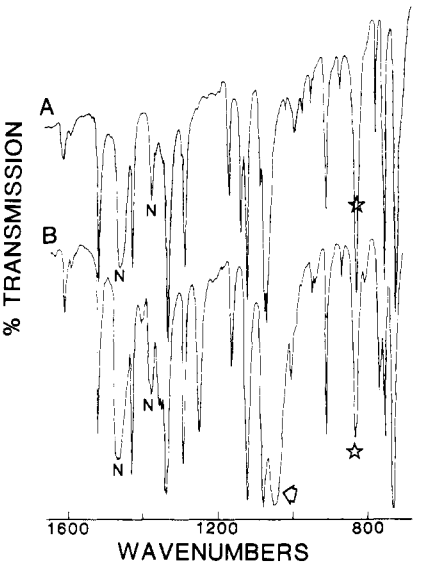

Figure 2. Infrared spectra (Nujol mulls) of (A) $Si(Pc)(OH)_2$ and (B) $Si(Pc)\{OSi[C(CH_3)_3](CH_3)_2\}_2$ (N = Nujol; star = mode which is predominantly (Pc)Si–O stretching; arrow = mode which is predominantly $[C(CH_3)_3](CH_3)_2Si$–O stretching).

necessary to achieve reasonable yields of analytically pure materials.

From optical, infrared, and 270-MHz ^{1}H NMR structure–spectra correlations (vide infra) as well as from elemental analyses, several crucial methodological considerations became evident. *Complete* hydrolysis of $Si(Pc)Cl_2$ and $Cl[Si(Pc)O]_2H$ (**4**) to the corresponding dihydroxides (Scheme I) could only be achieved by repeated grinding and hydrolysis sequences in the former case and grinding and prolonged hydrolysis in the latter (see Experimental Section for details). Complete "capping" of the resulting dihydroxide could only be ensured by using substantial excesses of $Si[C(CH_3)_3](CH_3)_2Cl$. In our hands, carrying out $Si[C(CH_3)_3](CH_3)_2Cl$ "capping" reactions in refluxing quinoline was less than optimal since this solvent is difficult to dry and undergoes significant decomposition at the reflux temperature (238 °C). Cleaner reactions were obtained at reflux in pyridine, which is far easier to dry and can be readily removed in vacuo. Under these conditions, dicapped monomer **3a** was isolated in analytical (and spectroscopic) purity after simple filtration and washing. Dicapped dimer **2a** could be isolated in ca. 90% purity by fractional precipitation from acetone. Further purification could be achieved by fractional crystallization from hot toluene, vacuum sublimation at 300–340 °C (substantial decomposition occurs, but a very pure product is obtained), or by size exclusion chromatography (Biobeads S-X8 eluting with 1:1 benzene/heptane). As inferred spectroscopically (see Experimental Section for details), halting the reaction sequence for **2a** at the appropriate place results in reasonably pure samples of **4** or **5**.

Both **2a** and **3a** are most soluble in basic organic solvents such as pyridine and quinoline, somewhat less soluble in polar solvents such as $CHCl_3$, CH_2Cl_2, chlorobenzene, THF, and DMF, less soluble still in benzene and mesitylene, and nearly insoluble in acetone and diethyl ether. Approximate solubilities of **2a** in dry benzene and dry CH_2Cl_2 are 15.0 and 280 μM, respectively. Monomer **3a** is less soluble, with approximate solubilities of 8.3 and 130 μM, respectively, in the same solvents. As monitored by ^{1}H NMR spectroscopy, solutions of **2a** and **3a** are inert to air and added water over periods of many days; i.e., neither $Si[C(CH_3)_3](CH_3)_2OH$ nor other new signals are observed.

Characterization and Structures of 2a and 3a. Spectroscopic Properties. Infrared spectroscopy was useful in identifying synthetic intermediates, assessing product purity, and in characterizing axial ligand monomer → dimer → polymer relationships of ultimate interest in studies of electron–phonon coupling. Complete infrared data for various monomeric, dimeric, and polymeric $Si(Pc)X_2$ species are set out in Table II. The numbering scheme

(24) (a) Berkowitz, J. *J. Chem. Phys.* **1979**, *70*, 2819–2828. (b) Ciliberto, E.; Fragalà, I.; Marks, T. J., manuscript in preparation.

(25) Kitagawa, S.; Morishima, I.; Yonezawa, I.; Sata, N. *Inorg. Chem.* **1979**, *18*, 1345–1349.

(26) (a) Ritter, G. W., II; Kenney, M. E. *J. Organomet. Chem.* **1978**, *157*, 75–79. (b) Mooney, J. R.; Choy, C. K.; Knox, K.; Kenney, M. E. *J. Am. Chem. Soc.* **1975**, *97*, 3033–3038. (c) Esposito, J. N.; Lloyd, J. E.; Kenney, M. E. *Inorg. Chem.* **1966**, *5*, 1979–1984.

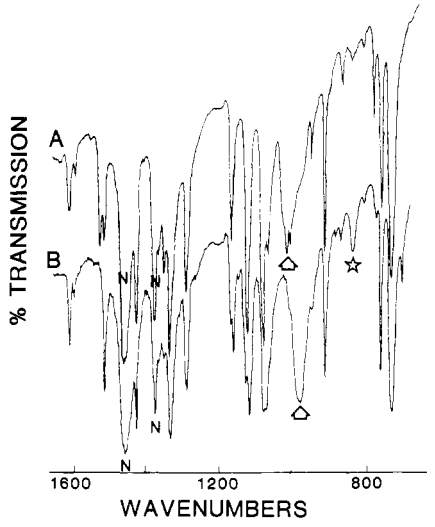

Figure 3. Infrared spectra (Nujol mulls) of (A) HOSi(Pc)OSi(Pc)Cl (**4**) and (B) HO[Si(Pc)O]$_2$H (**5**) (N = Nujol; star = mode which is predominantly (Pc)Si–O stretching; arrow = mode which is predominantly antisymmetric (Pc)Si–O–Si(Pc) stretching).

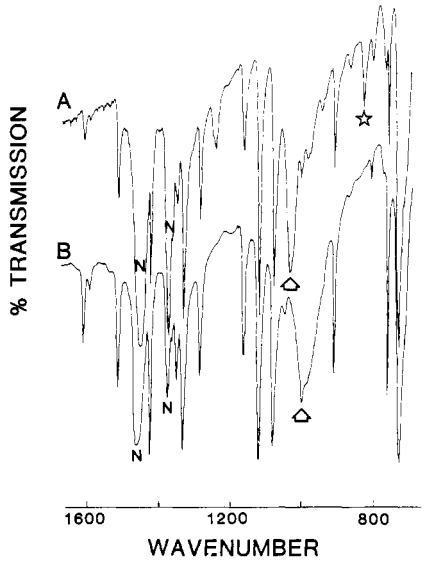

Figure 4. Infrared spectra (Nujol mulls) of (A) [C(CH$_3$)$_3$](CH$_3$)$_2$SiO-[Si(Pc)O]$_2$Si(CH$_3$)$_2$[C(CH$_3$)$_3$] (**2a**) and (B) [Si(Pc)O]$_n$ (N = Nujol; star = mode which is predominantly (Pc)Si–O stretching; arrow = mode which is predominantly antisymmetric (Pc)Si–O–Si(Pc) stretching).

of Sidorov and Kotlyar[10b,27] is employed to assign metal ion sensitive and metal ion insensitive M(Pc) skeletal modes. Assignments of key axial ligand-centered transitions in the present compounds are aided by previous M(Pc)X$_2$, [M(Pc)^{16}O]$_n$, [M(Pc)^{18}O]$_n$ (M = Si, Ge, Sn; X = Cl, ^{16}OH, ^{18}OH),[5b] Ge(Pc)-{OSi[C(CH$_3$)$_3$](CH$_3$)$_2$}$_2$,[28] [C(CH$_3$)$_3$](CH$_3$)$_2$SiO[Ge(Pc)O]$_2$Si-(CH$_3$)$_2$[C(CH$_3$)$_3$],[28] and group 4A hemiporphyrazine studies.[29] In Table III are compiled data useful for identifying Si[C-(CH$_3$)$_3$](CH$_3$)$_2$O-associated vibrations, and Figures 2–4 illustrate selected spectral regions. The axial SiO–H stretching frequency[29,30] is assigned at 3500 cm^{-1} in **3a**, **4**, and **5**. It is particularly useful in monitoring the course of Si–Cl hydrolysis, capping, or polymerization processes. In Si(Pc)Cl$_2$, the antisymmetrically

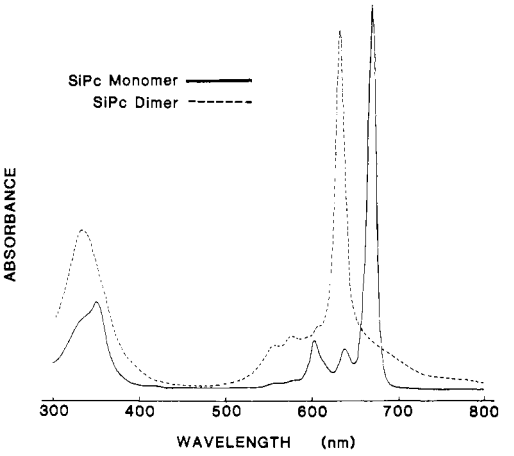

Figure 5. Optical absorption spectra of Si(Pc){OSi[C(CH$_3$)$_3$](CH$_3$)$_2$}$_2$ (**3a**) and [C(CH$_3$)$_3$](CH$_3$)$_2$SiO[Si(Pc)O]$_2$Si(CH$_3$)$_2$[C(CH$_3$)$_3$] (**2a**) as solutions in benzene.

coupled Si–Cl stretching frequency was assigned to a doublet at 468 and 430 cm^{-1} (presumably split by solid state effects);[5b,29] in **4**, a single transition at 465 cm^{-1} is most likely the Si–Cl stretch.

The antisymmetrically coupled (Pc)Si–O stretch in Si(Pc)(^{16}OH)$_2$ has been assigned at 830 cm^{-1} (808 cm^{-1} in Si(Pc)(^{18}OH)$_2$[5b]). Interestingly, a virtually unshifted transition can be assigned to an analogous, predominantly (Pc)Si–O mode in **3a**, **4**, **5**, and **2a** (Table II, Figures 2–4). From this information and Figure 3, the internal, antisymmetrically coupled (Pc)Si–O–Si(Pc) stretching mode can be assigned at 1000 cm^{-1} for **4** and at 984 cm^{-1} for **5**. On the basis of Figures 2 and 4, Table III, and literature data on siloxanes, a reasonable assignment of the predominantly [C(CH$_3$)$_3$](CH$_3$)$_2$Si–O stretching mode[31] is in the 1035–1050 cm^{-1} region. From Figure 4A, it appears that in **2a** this mode substantially overlaps the antisymmetric (Pc)Si–O–Si(Pc) stretching transition, which is observed as a strong, low-energy shoulder. One significant result that emerges from the foregoing discussion is that treating the [Si(Pc)^{16}O]$_n$ Si–O mode at 1000 cm^{-1} (950 cm^{-1} in [Si(Pc)^{18}O]$_n$) as a "local" antisymmetric (Pc)Si–O–Si(Pc) oscillator is energetically a reasonable first approximation (i.e., kinematic coupling between (Pc)Si–O modes appears to be small).

Solution optical spectra of **3a** and 2a are illustrated in Figure 5; full optical data for the compounds relevant to the present study are compiled in Table IV. The spectra features of **2a** and **3a** are essentially independent of solvent and independent of concentration over a tenfold range. All Si(Pc)X$_2$ spectra feature intense optical transitions in the 600–700 and 300–400 nm regions which, as has been noted previously, are analogous to porphyrin "Q-band" and "Soret band" π–π^* transitions, respectively.[10b,33,34] Discussion of the orbitals involved in these transitions is deferred until the DV-Xα results are presented. Weaker spectral features to the high energy of the "Q band" are generally believed to be vibronic in origin. Two empirical features of the present spectra are noteworthy and are particularly useful for monitoring the course of the syntheses. First, substitution of axial (Pc)SiCl for (Pc)SiO– invariably results in a higher energy shift of the Q band while the

(27) (a) Sidorov, A. N.; Kotlyar, I. P. *Opt. Spektrosk.* **1961**, *11*, 175–184. (b) Kobayashi, T.; Kurokawa, F.; Uyeda, N.; Suito, E. *Spectrochim. Acta, Part A* **1970**, *26A*, 1305–1311. (c) Stienbach, F.; Joswing, H.-J. *J. Chem. Soc., Faraday Trans. 1* **1979**, *75*, 2594–2600.

(28) Doris, K. A.; Marks, T. J., manuscript in preparation.

(29) Dirk, C. W.; Marks, T. J. *Inorg. Chem.*, in press.

(30) (a) Kantor, S. W. *J. Am. Chem. Soc.* **1953**, *75*, 2712–2714. (b) Licht, K.; Kriegsman, H. *Z. Anorg. Allg. Chem.* **1963**, *323*, 190–206. Rouviere, J.; Tobacik, V.; Leury, G. *Spectrochim. Acta, Part A* **1973**, *29A*, 229–242.

(31) (a) Smith, A. L. "Analysis of Silicones"; Wiley: New York, 1974; pp 275–279. (b) Rappoport, Z. "Handbook of Tables for Organic Compounds Identification"; CRC Press: Cleveland, OH, 1967; pp 441–449.

(32) For discussions of dispersion relation optical branch descriptions and approximations in polymer vibrational spectroscopy, see: (a) Koenig, J. L. "Chemical Microstructure of Polymer Chains"; Wiley-Interscience: New York, 1980; Chapter 7. (b) Turrell, G. "Infrared and Raman Spectra of Crystals"; Academic Press: New York, 1972; Chapters 3 and 7.

(33) (a) Marks, T. J.; Stojakovic, D. R. *J. Am. Chem. Soc.* **1978**, *100*, 1695–1705 and references therein. (b) Gouterman, M. In "The Porphyrins"; Dolphin, D., Ed.; Academic Press: New York, 1978; Vol. 3, Part A, pp 1–163.

(34) (a) Shaffer, A. M.; Gouterman, M.; Davidson, E. R. *Theor. Chim. Acta* **1973**, *30*, 9–30. (b) Schaffer, A. M.; Gouterman, M. *Ibid.* **1972**, *25*, 62–70. (c) Edwards, L.; Gouterman, M. *J. Mol. Spectrosc.* **1970**, *33*, 292–310. (d) Chen. I. *Ibid.* **1967**, *23*, 131–143.

Table II. Infrared Spectral Data for Monomeric, Dimeric, and Polymeric Phthalocyaninatosilicon Species

	$Si(Pc)Cl_2$	$Si(Pc)(OH)_2$	$Si(Pc)(OR)_2$ (**3a**)	HOSi(Pc)OSi(Pc)Cl (**4**)	HO[Si(Pc)-O]$_2$H (**5**)	ROSi(Pc)OSi-(Pc)OR (**2a**)	$[Si(Pc)O]_n$
	323 s						
	418 m		424 m	415 s	415 s		
	430 s						
1[b]	438 sh	450 w	436 s	450 w	450 w		
	468 vs			465 w			
2	509 w						
	533 s	530 m	530 s	530 s	530 s	530 m	530 m
3	574 m	575 m	562 m, 575 m	575 m	575 s	575 m	575 m
	609 w	617 w		610 vw			
4	647 m	644 m	630 w, 645 w	635 vw	643 m	645 w	646 w
				647 w			
		674 w	674 w	675 vw, sh	675 m		
	692 m	701 w	698 w	697 vw, sh	700 m		
5	730 vs	728 vs	733 vs	732 vs	728 vs	729 vs	721 vs
6	760 s	758 vs	758 s	760 s	758 vs	759 s	759 vs
							762 vs
8	774 w	775 w		774 w	774 w	768 w	
9	783 s	780 s	770 s	780 m			
10	808 w	804 sh	810 vw	808 w	804 w	804 w	804 w
		830 vs	832 vs	835 w, br	832 br, m	830 m	
11	867 m	872 w	869 w	865 m	867 w	867 w	869 vw
12	882 m	875 w			880 vs		
13	912 s	911 m	910 s	912 s	910 s	910 s	910 s
14			940 w		946 sh		936 vs
15		951 w	950 w			948 vw	
	960 m			950 m			
	987 w	976 w	975 w, sh	1000 s, vbr	984 s, br		978 s, bd
	1004 w	991 w	1003 m			987 w	1000 s, br
		1020 w		1010 w, 1018 m		1004 w	
	1050 sh		1050 vs, br			1035 vs, br	1043 w
17	1060 s	1072 vs	1072 sh	1072 sh	1072 s		
18	1080 vs	1078 vs	1079 vs	1085 vs	1078 s	1080 vs	1080 vs
		1089 m			1082 m		
20	1120 vs	1119 s	1120 vs	1125 vs	1119 s	1121 vs	1121 vs
		1134 m			1130 m		
21	1162 s	1166 m	1166 m	1170 s	1164 s	1165 s	1164 s
					1170 sh		1170 sh
							1192 w
	1240 vw	1223 w	1239 s			1244 m, bd	
23	1290 s	1290 s	1290 s	1292 s	1289 s	1290 s	1289 s
26	1336 vs	1335 vs	1343 vs	1338 vs	1335 vs	1334 vs	1334 vs
	1342 sh		1350 m, sh				
	1352 sh		1367 m, sh	1352 sh	1352 sh	1353 m, sh	1351 m
27	1430 s	1431 s	1404 w, 1430 s	1430 s	1428 vs	1427 s	1426 vs
30	1532 s	1518 s	1518 s	1518 m, 1529 m	1517 s	1518 s	1517 s
31	1595 sh	1595 w	1595 vw	1596 w, sh	1597 w	1596 vs	1596 w
32	1610 m	1609 m	1610 m	1611 m	1614 m	1614 m	1614 m
		~3500 s		~3500 w	~3500 m		

[a] In cm^{-1}; s = strong, m = medium, br = broad, sh = shoulder, v = very. R = $Si[C(CH_3)_3](CH_3)_2$. [b] Pc skeletal mode numbering according to mode assignments of ref 10b; with system derived from ref 27a.

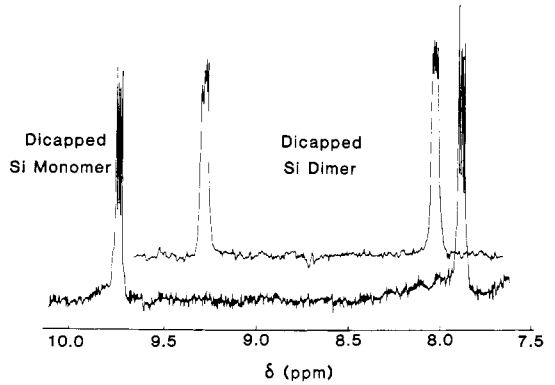

Figure 6. ^1H NMR spectra (270 MHz) of the aromatic regions of $Si(Pc)\{OSi[C(CH_3)_3](CH_3)_2\}_2$ (**3a**) and $[C(CH_3)_3](CH_3)_2SiO[Si(Pc)-O]_2Si(CH_3)_2[C(CH_3)_3]$ (**2a**) in C_6D_6.

Soret is essentially unchanged. This effect is insensitive to solvent and the oxygen substituent (H or capping group). Similar effects on M(Pc) spectra as a function of M are frequently associated with electronegativity trends.[5b,35] A second effect is the high-energy shift of the Q band (ca. 30 nm) upon cofacial dimer formation. This effect has previously been noted in a related cofacial Si(Pc) system[36] and has been qualitatively explained via excitonic, through-space coupling of the adjacent transition dipoles, which are polarized in the plane of the macrocyclic ring; this effect is portrayed schematically[37] in A. Shifts of macrocycle π–π*

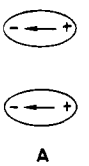

A

transitions upon association is well-known for phthalocyanines,[38]

(35) (a) Gouterman, M.; Schwarz, R. F.; Smith, P. D.; Dolphin, D. *J. Chem. Phys.* **1973**, *59*, 676–690. (b) Gouterman, M. *J. Chem. Phys.* **1959**, *30*, 1139–1161. (c) Gouterman, M.; Holten, D.; Lieberman, S. *Chem. Phys.* **1977**, *25*, 139–153.

(36) Hush, N. S.; Woolsey, J. S. *Mol. Phys.* **1971**, *21*, 465–474.

(37) Torrance, J. B.; Scott, B. A.; Welber, B.; Kaufman, F. B.; Seiden, P. E. *Phys. Rev. B: Condens. Matter* **1979**, *19*, 730–741.

Table III. Infrared Spectral Data (cm^{-1}) for $Si[C(CH_3)_3](CH_3)_2X$ and Related Compounds

$Si(CH_3)_3Cl$	$[Si(CH_3)_3]_2O$	$Si[C(CH_3)_3](CH_3)_2Cl$	$Si[C(CH_3)_3](CH_3)_2OH$
			355 w
		485 s	397 w
	522 w, bd		
	600 w	587 m	568 m
632 s	619 s		666 s
	688 s	680 m	
694 m			
		720 w	722 w
758 s	758 s	781 s	774 vs, bd
	820–860 vs, bd	803 s	811 sh
		821 s	820–870 vs, bd
		840 s	
843 vs, bd			
		938 w	949 m
		1005 vw	
1050 w, bd	1000–1150 vs, bd		1006 m
		1000–1110 w, bd	970–1100 m, bd
1253 vs	1253 s	1253 s	1255 vs
1335 w	1304 vs, sh		
		1362 m, sh	1361 m
	1401 w, sh	1390 vs	1406 w
1410 m	1414 m	1408 vw	1406 w
1450 w, bd	1435–1452 m, bd		
	1580 m		
2950 m	2973 m		
	2982 s		
	3450 v, bd		3100–3500 vvs, bd
			3698 m

[a] Reference 16, p 1094. [b] Neat, KBr plates (all other Nujol mulls).

Table IV. Optical Absorption Data for Various Phthalocyaninatosilicon Compounds in Solution

compound	solvent	Q band, nm	Soret band, nm
$Si(Pc)Cl_2$	pyridine	699, (627)	367, 314
$Si(Pc)(OH)_2$	pyridine	671, (641.5, 604)	
	THF	667, (636, 602)	(377), 363, 318
	$CHCl_3$	674.5, (644, 605)	357
	benzene	672, (642, 605)	355
$Si(Pc)(OR)_2$[b] (**3a**)	pyridine	670.5, (640, 604)	
	$CHCl_3$	668, (638, 602)	
	benzene	668.5, (638, 604)	353, 330 sh, bd
$Si(Pc)(OR')_2$[c]	THF	665, (634, 597, 574, 553)	352, 336, 287
$HO[Si(Pc)O]_2H$ (**5**)	pyridine	636, (580, 560)	332
	THF	630, (600, 575, 555)	328
	$CHCl_3$	634, (605, 577, 557)	331.5, 282
ROSi(Pc)OSi(Pc)-OR (**2a**)[b]	pyridine	635, (608 sh, 574, 555)	332
	THF	630, (603 sh, 574, 554)	331
	$CHCl_3$	634, (605 sh, 574, 554)	330
	benzene	633, (606 sh, 574, 554)	332
R'OSi(Pc)OSi(Pc)-OR'[c]	THF	628, (604 sh, 574, 554)	331, 282.5

[a] Peaks of smaller intensities are listed in parentheses and discussed in the text. [b] R = $Si[C(CH_3)_3](CH_3)_2$–. This work. [c] R' = $Si[OSi(CH_3)_3]_2(CH_3)$–. Data from ref 36.

porphyrins,[38,39] and chlorophylls.[40] Interestingly, however, the shift is most frequently to lower energy for the "Q-band"-like transition, reflecting structural differences in the cofacial association (e.g., "slipped" rather than D_n) as well as transition dipole magnitude and substituent electronegativity/polarizability effects.[35c] Further clarification of the optical spectral assignments will follow the presentation of the DVM-Xα calculations (vide infra).

Table V. ^1H NMR Data for Various $Si(Pc)X_2$ Monomers and Dimers

compound	solvent	assign	δ	integrated area[a]
$Si(Pc)(OR)_2$[b] (**3a**)	C_6D_6	3,6 Pc	9.75	8.0 (8.0)
		4,5 Pc	7.87	11.1 (8.0)
		methyl	−2.69	11.0 (12.0)
		tert-butyl	−1.28	20.9 (18.0)
$Si(Pc)(OR)_2$[b] (**3a**)	$CDCl_3$	3,6 Pc	9.66	
		4,5 Pc	8.34	
		methyl	−2.97	
		tert-butyl	−1.43	
$Si(Pc)(OR')_2$[c]	CCl_4	3,6 Pc	9.63	
		4,5 Pc	8.30	
		"outer" Me	−1.25	
		"inner" Me	−2.90	
$Si(Pc)(OR'')_2$[d]	CCl_4	3,6 Pc	9.68	
		4,5 Pc	8.35	
		ethyl, CH_3	−1.25	
		ethyl, CH_2	−2.48	
ROSi(Pc)OSi(Pc)OR[b] (**2a**)	C_6D_6	3,6 Pc	9.26	8.0 (8.0)
		4,5 Pc	8.00	8.4 (8.0)
		methyl	−3.78	6.0 (6.0)
		tert-butyl	−2.16	9.1 (9.0)
ROSi(Pc)OSi(Pc)OR[b] (**2a**)	$CDCl_3$	3,6 Pc	9.00	8.0 (8.0)
		4.5 Pc	8.30	8.4 (8.0)
		methyl	−4.08	5.7 (6.0)
		tert-butyl	−2.32	8.8 (9.0)
R'OSi(Pc)OSi(Pc)OR'[c]	CCl_4	3,6 Pc	9.00	
		4,5 Pc	8.31	
		OSi-CH_3	−1.91	
		Si-CH_3	−4.0	

[a] Theoretical values are in parentheses. Experimental areas are considered accurate to ±10%. [b] R = $Si[C(CH_3)_3](CH_3)_2$–. This work. [c] R' = $Si[OSi(CH_3)_3]_2(CH_3)'$. Data of ref 42. [d] R'' = $Si(C_2H_5)_3'$. Data of ref 42.

With careful integration, high-field ^1H NMR spectroscopy provides quantitative information on both monomer/dimer content and degree of capping. Representative spectra are illustrated in Figure 6, while data for the present and closely related complexes[41]

(38) (a) Konishi, S. ; Hoshino, M.; Imamura, M. *J. Phys. Chem.* **1982**, *86*, 4888–4892. (b) Davidson, A. T. *J. Chem. Phys.* **1982**, *77*, 168–172. (c) Abkowitz, M.; Monahan, A. R. *J. Chem. Phys.* **1973**, *58*, 2281–2287.

(39) Collman, J. P.; Bencosme, C. S.; Barnes, C. E.; Miller, B. D. *J. Am. Chem. Soc.* **1983**, *105*, 2704–2710 and references therein.

(40) Smith, K. M.; Kehres, L. A.; Fajer, J. *J. Am. Chem. Soc.* **1983**, *105*, 1387–1389 and references therein.

Table VI. Atomic Coordinates, Equivalent Isotropic Temperature Factors for Ordered Non-Hydrogen Atoms, and Isotropic Temperature Factors for Disordered (cap) Atoms and Hydrogens in **2a**

atom[a]	x^b	y^b	z^b	$U_{eq}{}^c$ Å^2	atom[a]	x^b	y^b	z^b	$U_{eq}{}^c$ Å^2
Si(1)	4362 (2)	2411 (3)	2100 (2)	41 (2)	C(27)	5755 (8)	3255 (17)	147 (8)	75 (15)
O(1)	5000	2401 (9)	2500	37 (8)	C(28)	5949 (10)	4147 (18)	−83 (9)	83 (16)
O(2)	3717 (4)	2440 (7)	1704 (4)	54 (6)	C(29)	5829 (11)	5006 (19)	167 (10)	101 (18)
N(1)	4640 (6)	4736 (9)	1733 (7)	55 (9)	C(30)	5471 (9)	5081 (13)	660 (9)	72 (14)
N(2)	4130 (6)	3669 (8)	2427 (6)	46 (8)	C(31)	5225 (7)	4243 (10)	916 (7)	55 (11)
N(3)	3533 (6)	3169 (11)	3252 (6)	60 (9)	C(32)	4862 (7)	4045 (10)	1414 (6)	39 (9)
N(4)	3929 (5)	1768 (9)	2722 (5)	43 (8)	Si(2)A	3102 (5)	2013 (8)	1385 (5)	7 (0)
N(5)	4097 (7)	90 (10)	2479 (8)	68 (11)	Si(2)B	322 (1)	274 (2)	116 (1)	6 (1)
N(6)	4572 (6)	1139 (8)	1775 (5)	43 (8)	Si(2)C	296 (1)	242 (2)	163 (1)	10 (1)
N(7)	5130 (6)	1632 (8)	925 (5)	53 (8)	C(33)A	325 (2)	125 (3)	73 (2)	9 (1)
N(8)	4805 (5)	3031 (8)	1471 (5)	44 (7)	C(34)A	265 (2)	122 (2)	194 (2)	5 (1)
C(1)	4299 (7)	4528 (11)	2183 (9)	58 (12)	C(35)A	251 (3)	325 (5)	134 (3)	16 (3)
C(2)	4052 (9)	5315 (11)	2554 (10)	73 (14)	C(36)A	298 (2)	395 (3)	89 (2)	8 (1)
C(3)	4116 (11)	6292 (1)	2516 (12)	94 (19)	C(37)A	237 (2)	349 (4)	190 (2)	8 (2)
C(4)	3767 (14)	6798 (19)	2974 (15)	126 (23)	C(38)A	200 (1)	279 (2)	87 (1)	6 (1)
C(5)	3386 (10)	6434 (18)	3394 (10)	88 (17)	C(33)B	331 (3)	205 (5)	46 (3)	6 (2)
C(6)	3388 (9)	5355 (15)	3390 (10)	79 (15)	C(34)B	329 (5)	379 (8)	77 (5)	12 (4)
C(7)	3696 (7)	4872 (12)	2969 (8)	50 (11)	C(33)C	243 (4)	138 (6)	168 (4)	8 (3)
C(8)	3763 (8)	3838 (12)	2920 (7)	51 (12)	C(34)C	255 (5)	287 (8)	118 (5)	11 (4)
C(9)	3633 (8)	2212 (12)	3165 (7)	51 (11)	C(35)C	240 (4)	311 (7)	211 (4)	6 (3)
C(10)	3380 (8)	1504 (14)	3571 (8)	63 (13)	H(3)	444 (7)	675 (12)	242 (7)	7 (5)
C(11)	3074 (9)	1607 (16)	4096 (9)	65 (14)	H(4)	372 (7)	728 (11)	291 (7)	6 (5)
C(12)	2947 (11)	727 (22)	4335 (11)	102 (21)	H(5)	312 (11)	688 (17)	369 (11)	9 (10)
C(13)	3074 (12)	−208 (15)	4137 (10)	89 (18)	H(6)	293 (7)	516 (12)	357 (7)	10 (6)
C(14)	3354 (12)	−255 (16)	3627 (11)	88 (18)	H(11)	301 (10)	235 (16)	420 (10)	13 (10)
C(15)	3524 (8)	592 (15)	3344 (8)	61 (12)	H(12)	281 (7)	71 (12)	463 (6)	2 (6)
C(16)	3874 (8)	780 (11)	2823 (8)	56 (12)	H(13)	295 (9)	−85 (15)	438 (9)	13 (8)
C(17)	4407 (9)	268 (12)	2004 (7)	61 (12)	H(14)	359 (8)	−79 (13)	345 (8)	7 (7)
C(18)	4640 (7)	−469 (10)	1620 (7)	50 (11)	H(19)	445 (5)	−176 (8)	185 (4)	3 (3)
C(19)	4618 (11)	−1469 (18)	1645 (12)	106 (20)	H(20)	483 (8)	−278 (14)	122 (8)	11 (9)
C(20)	4885 (12)	−2038 (15)	1193 (13)	97 (19)	H(21)	537 (9)	−201 (16)	40 (9)	10 (9)
C(21)	5169 (11)	−1579 (15)	747 (11)	91 (17)	H(22)	541 (5)	−37 (8)	49 (5)	3 (4)
C(22)	5202 (10)	−601 (16)	720 (10)	73 (17)	H(27)	585 (6)	256 (11)	0 (6)	5 (5)
C(23)	4920 (8)	−26 (11)	1158 (7)	51 (11)	H(28)	620 (7)	398 (11)	−43 (7)	4 (5)
C(24)	4869 (6)	998 (10)	1273 (6)	40 (9)	H(29)	603 (5)	552 (8)	12 (4)	6 (3)
C(25)	5103 (7)	2588 (12)	1030 (6)	53 (9)	H(30)	540 (5)	570 (9)	90 (5)	2 (4)
C(26)	5404 (7)	3331 (12)	656 (7)	55 (11)					

[a] Numbering scheme is seen in Figure 8. [b] $\times 10^4$ for ordered non-hydrogen atoms and Si(2)A; $\times 10^3$ for disordered atoms and hydrogens. [c] $U_{eq} = {}^1/_3$ tr(U); U_{iso} (Å^2) = $(1/8\pi^2)B_{iso}$. [d] Atoms designated A have 50% occupancy, with B and C each having 25% occupancy.

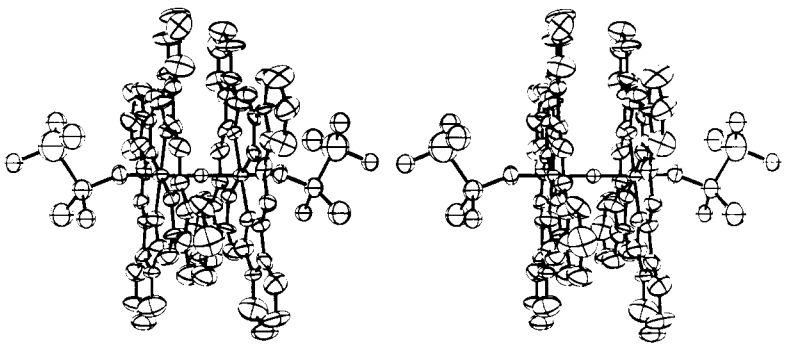

Figure 7. Stereoview of the molecular structure of $[C(CH_3)_3](CH_3)_2SiO[Si(Pc)O]_2Si(CH_3)_2[C(CH_3)_3]$ (**2a**) seen perpendicular to the Si–O–Si axis. Vibrational ellpsoids are drawn at the 50% probability level.

are set out in Table V. As has already been demonstrated,[33a] M(Pc) benzo proton chemical shift displacements can be readily understood in terms of shielding arising from a combination of local magnetic anisotropy and from classical ring current-based magnetic induction. The simple AA′BB′ patterns observed for **2a** in the present case suggest a static dimer structure of D_{4h} or D_{4d} symmetry or that there is rapid (on the NMR time scale) Pc ring rotation about the Si–O axes. Solid-state diffraction results suggest the latter (vide infra).

Molecular Structure of $[C(CH_3)_3](CH_3)_2SiO[Si(Pc)O]_2Si(CH_3)_2[C(CH_3)_3]$ (2a). Single crystals of **2a** suitable for X-ray diffraction were obtained by slow evaporation of chloroform solutions. Details of data collection and refinement are summarized in Table I, while Table VI presents final atomic coordinates and isotropic temperature factors and Table VII,[22] anisotropic temperature factors. A stereoview of **2a** is shown in Figure 7, while a view along the Si–O–Si axis and the atom numbering scheme are shown in Figure 8. Although solution of the crystal structure was complicated somewhat by disorder of the $-Si[C(CH_3)_3](CH_3)_2$ capping groups, the configuration of the basic (Pc)Si–O–Si(Pc) core is satisfactorily determined. In Table VIII are set out metrical parameters for **2a** averaged according to chemically equivalent bonds. The simplified atom labeling scheme for conveying this information is shown in B. For purposes of comparison, the data for **2a** are compared to corresponding averaged M(Pc) (M = Mg, Zn, Fe, Mn, Ni)[42-45] and Si(Pc)$(OR)_2$ (R =

(41) Janson, T. R.; Kane, A. R.; Sullivan, J. F.; Knox, , K.; Kenney, M. E. *J. Am. Chem. Soc.* **1969**, *91*, 5210–5214.

(42) Fischer, M. S.; Templetron, D. H.; Zalkin, A.; Calvin, M. *J. Am. Chem. Soc.* **1971**, *93*, 2622–2628.

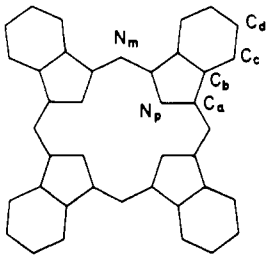

B

$Si(CH_3)_3$[26b] metrical parameters. It can be seen that the internal Si(Pc) structural parameters in **2a** are unexceptional for a metallophthalocyanine contiaining a first-row transition-metal ion, Mg^{2+}, or Si^{4+}.

As can be seen in Figures 7 and 8, the molecular structure of **2a** is that of a cofacially linked dimer, as intended. In the solid state, there is a crystallographic twofold axis perpendicular to the Si–Si interatomic vector and passing through bridging oxygen atom O(1). Although the phthalocyanine macrocycles are not constrained to be planar by the crystallographic symmetry, they are nearly so and are parallel to the two-fold axis. The largest deviation from planarity of any atom in the Pc rings is about 0.27 Å.[46] Individual subunits of the Pc ring, the pyrrole rings and benzo units, are planar to within 0.04 Å. The dihedral angles between an individual pyrrole unit and the associated fused benzo substituent are all less than 2.8°. Within experimental error, the silicon atom is in the plane of the four coordinating nitrogen atoms and the Si–Si vector is perpendicular to the phthalocyanine least-squares mean plane.

The Si–O–Si angle in **2a** is essentially linear at 179 (1)°. Linear Si–O–Si functionalities are common in certain classes of siloxanes (R_3Si–O–SiR_3)[47] and silicates.[48] The (Pc)Si–O–SiR_3 angle in **2a** is 157.2 (5)° (for the capping group with 50% occupancy), which compares favorably with angles of 157.8 (1)° and 156.6 (1)° in $Si(Pc)[OSi(CH_3)_2]_2$.[26b] The Si–Si distance of 3.32 (1) Å in **2a** [Si–O = 1.661 (4) Å] represents the ring–ring interplanar spacing and agrees well with the value of 3.33 (2) Å derived for $[Si(Pc)O]_n$ on the basis of a computer-aided analysis of powder diffraction data.[10b] The present (Pc)Si–OSi(cap) and (Pc)SiO–Si(cap) distances of 1.670 (10) and 1.630 (10) Å, respectively, compare well with corresponding distances of 1.679 (2) and 1.606 (2) Å (av) in $Si(Pc)[OSi(CH_3)_3]_2$.[26b] Reference to Figure 8 reveals that the Pc rings in **2a** are not in an eclipsed conformation but are staggered by 36.6°. This result is in good agreement with a staggering angle of 39 (3)° derived for $[Si(Pc)O]_n$ in the aforementioned powder diffraction analysis[10b] and an angle of 39.6° reported for adjacent, stacked $Ni(Pc)^{0.33+}$ units in Ni(Pc)I.[45] In general, staggering angles in (macrocycle)M–X–M(macrocycle) systems[10b,45,46b,49–51] appear to be a sensitive function of interplanar spacing and macrocycle substituents. These trends are evident in Table IX; staggering angles near 0° have only been observed in cases of relatively large interplanar separations ($[Ga(Pc)F]_n$,[49] $[Ge(Pc)O]_n$[10b]) while ring substituent steric effects are clearly most important in $[Mo(TTP)Cl]_2O$,[51] TTP = *meso*-tetra-*p*-

Table VIII. Averaged Bond Lengths (Å) and Angles in Crystalline $[C(CH_3)_3](CH_3)_2SiO[Si(Pc)O]_2Si(CH_3)_2[C(CH_3)_3]$, **2a**,[a] Typical Metallophthalocyanines,[b] and $Si(Pc)[OSi(CH_3)_3]_2$.[c]

	2a[a]	mean M(Pc)[b]	$Si(Pc)[OSi(CH_3)_3]_2$[c]
		Bond[a]	
N_p–C_a	1.37 (2)	1.377 (10)	1.375 (4)
N_m–C_a	1.31 (2)	1.326 (7)	1.321 (4)
C_a–C_b	1.45 (2)	1.453 (3)	1.449 (4)
C_b–C_c	1.38 (2)	1.393 (2)	1.391 (3)
C_b–C_b	1.39 (2)	1.394 (4)	1.386 (5)
C_c–C_d	1.40 (4)	1.386 (7)	1.380 (6)
C_d–C_d	1.36 (4)	1.395 (2)	1.386 (12)
		Angle	
C_a–N_p–C_a	109 (1)	107.7 (8)	107.2 (4)
N_p–C_a–C_b	109 (1)	109.6 (4)	109.8 (3)
C_a–C_b–C_b	107 (1)	106.6 (3)	106.6 (2)
C_a–C_b–C_c	132 (2)	132.3 (2)	131.9 (4)
C_b–C_c–C_d	117 (2)	117.4 (2)	116.7 (4)
C_d–C_d–C_c	122 (2)	121.5 (1)	121.5 (1)
C_b–C_b–C_c	121 (2)	121.2 (2)	121.6 (4)
N_p–C_a–N_m	128 (1)	127.9 (1)	127.9 (2)
C_a–N_m–C_a	122 (1)	122.4 (5)	121.5 (1)

[a] Labeling scheme as shown in B. [b] Averaged values from the solid state structures of Mg(Pc),[42] Zn(Pc),[43] Fe(Pc),[44] Mn(Pc),[44] and $Ni(Pc)I_{1.0}$.[45] [c] Data of ref 26b.

Table IX. Adjacent Ring Staggering Angles (ϕ) and M–X–M Distances (d) in Some Cofacially Joined Metallomacrocycle Complexes[a]

compound	ϕ, deg	d, Å	ref
$[C(CH_3)_3](CH_3)_2SiO[Si(Pc)O]_2Si(CH_3)_2[C(CH_3)_3]$ (**2a**)	36.6 (-)	3.32 (1)	this work
$[Si(Pc)O]_n$	39 (3)	3.33 (2)	10b
$Ni(Pc)I_{1.0}$	39.6	3.244 (2)	45
$[Mn(Pc)(pyridine)]_2O$	41	3.42 (1)	50
$[Mo(TTP)Cl]_2O$[b]	30.4	3.702 (12)	51
$[Mn(TPP)N_3]_2O$[c]	28.5	3.537 (4)	52
$\{Si(CH_3)[OSi(CH_3)_3]_2\}O[Si(Pc)O]_3O\{Si(CH_3)[OSi(CH_3)_3]_2\}$	15.9	3.324 (2)	16b
$[Ge(Pc)O]_n$	0 (5)	3.53 (2)	10b
$[Ga(Pc)F]_n$	0	3.872 (2)	49

[a] Standard deviations given when reported in original literature. Interplanar spacing does not equal D(M–X–M) in cases of ring distortion. [b] TTP = *meso*-tetra-*p*-tolylporphyrinato. [c] TPP = *meso*-tetraphenylporphyrinato.

Table X. Photoelectron Spectroscopic Data and Assignments for $Si(Pc)[OSi[C(CH_3)_3](CH_3)_2]_2$ (**3a**)

band label[a]	IE, eV	DV-Xα eigenvalues,[b] eV	assignment	
a	6.46	6.46	$2a_{1u}$	
b	7.99	7.99	$19e_u$	
c	9.39	8.33	$6e_g$	
		8.49	$8b_{2g}$	+ σ(Si–C)
		8.57	$6a_{2u}$	
e	9.31	9.24	$18e_u$	

[a] As shown in Figure 9. [b] The values, calculated as orbital energies, have been multiplied by a scale factor to fit the separation of bands a and b. This scale factor takes relaxation effects into account, without the necessity for transition-state calculations (see text discussion on the monomer).

(43) Scheidt, W. R.; Dow, W. *J. Am. Chem. Soc.* **1977**, *99*, 1101–1104.
(44) Kirner, J. F.; Dow, W.; Scheidt, W. R. *Inorg. Chem.* **1976**, *15*, 1685–1689.
(45) Schramm, C. J.; Scaringe, R. P.; Stojakovic, D. R.; Hoffman, B. M.; Ibers, J. A.; Marks, T. J. *J. Am. Chem. Soc.* **1980**, *102*, 6702–6713.
(46) (a) An unpublished[46b,c] crystal structure of trimeric $\{Si(CH_3)[OSi(CH_3)_3]_2\}O[Si(Pc)O]_3\{Si(CH_3)[OSi(CH_3)_3]_2\}$ reveals linear Si–O–Si units, nearest-neighbor (Pc)Si–Si(Pc) distances of 3.324 (9) Å, staggering angles of 15.9° between adjacent rings, and a slight buckling of the two outer Pc rings in the trimer away from the interior ring. With the information at hand, it is not clear whether the buckling is a consequence of the reduced staggering angle, which itself reflects unusual intramolecular interactions with this different capping group and/or adventitious packing forces. (b) Swift, D. R. Ph.D Thesis, Case Western Reserve University, Cleveland, OH 1970. (c) For an ORTEP diagram of this structure, see ref 10h.
(47) (a) Glidewell, C.; Liles, D. C. *J. Organomet. Chem.* **1981**, *212*, 291–300 and refereneces therein. (b) Glidewell, C.; Liles, D. C. *J. Organomet. Chem.* **1979**, *174*, 275–279 and references therein.
(48) (a) Smolin, Yu. I.; Shepelev, Yu. F. *Acta Crystallogr., Sect. B* **1970**, *B26* 484–492. (b) O'Keefe, M.; Hyde, B. G. *Acta Crystallogr. Sect. B* **1978**, *B34*, 27–32 and references therein.
(49) Wynne, K. J.; Nohr, R. S. *J. Chem. Soc., Chem. Commun.* **1981**, 1210–1211.
(50) (a) Vogt, L. H., Jr.; Zalkin, A.; Templeton, D. H. *Inorg. Chem.* **1967**, *6*, 1725–1730. (b) Vogt, L. H., Jr.; Zalkin, A.; Templeton, D. H. *Science (Washington, DC)* **1966**, *15*, 569–570.
(51) Colin, J.; Chevrier, B.; De Cian, A.; Weiss, R. *Angew. Chem. Int. Ed. Engl.* **1983**, *22*, 247–248.

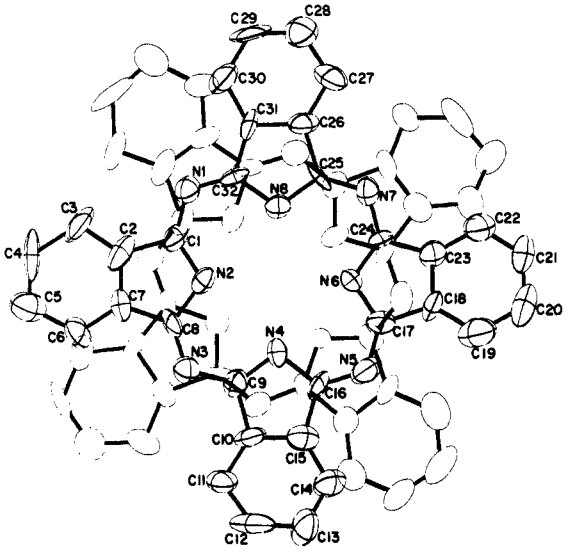

Figure 8. View of the molecular structure of $[C(CH_3)_3](CH_3)_2SiO[Si(Pc)O]_2Si(CH_3)_2[C(CH_3)_3]$ (**2a**) seen along the Si–O–Si axis. For clarity, the silicon atoms and axial ligands have been deleted, and the 50% probability ellipsoids for the cofacial phthalocyanine rings have been drawn differently.

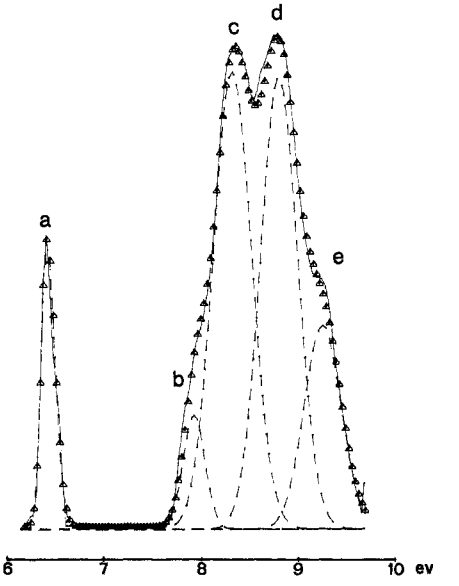

Figure 9. He I photoelectron spectrum of monomer $Si(Pc)\{OSi[C(CH_3)_3](CH_3)_2\}_2$ (**3a**) in the low ionization energy region. The triangles are experimental data points, the dashed lines are Gaussian spectral components, and the solid line, is convoluted components.

tolylporphyrinato, and $[Mn(TPP)N_3]_2O$,[52] TPP = *meso*-tetraphenylporphyrinato.

Photoelectron Spectroscopy of Compounds 3a and 2a. The gas-phase He I PES spectrum of $Si(Pc)\{OSi[C(CH_3)_3](CH_3)_2\}_2$ is shown in Figure 9, and data are complied in Table X. The spectrum exhibits a very narrow onset peak (a) followed by a structured band envelope (b–e). Although the same general features were reported in earlier PES studies of metallophthalocyanines,[13,24a] the high quality of the present data allows the first resolution of transitions b–e in the 7.5–10-eV envelope. Furthermore, a high-resolution scan (Figure 10) in the 6–7-eV region reveals a vibrational progression (ν = 1240 ± 200 cm^{-1}) on the higher ionization energy side of band a. The specific assignment of the PES data is deferred until the discussion of the electronic structure calculations (vide infra).

(52) Schardt, B. C.; Hollander, F. J.; Hill, C. L. *J. Am. Chem. Soc.* **1982**, *104*, 3964–3972.

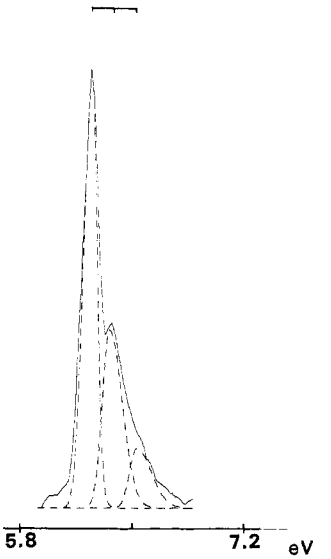

Figure 10. Expanded scale view of the onset band in the He I photoelectron spectrum of monomer $Si(Pc)\{OSi[C(CH_3)_3](CH_3)_2\}_2$ (**3a**).

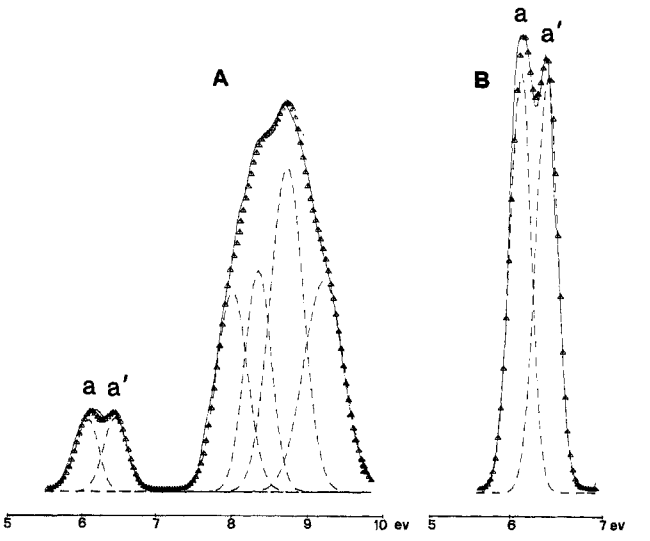

Figure 11. A. He I photoelectron spectrum of dimer $[C(CH_3)_3](CH_3)_2SiO[Si(Pc)O]_2Si(CH_3)_2[C(CH_3)_3]$ (**2a**) in the low ionization energy region. B. Expanded view of the onset doublet. Experimental data points are represented by triangles, Gaussian components by dashed lines, and convoluted components by solid lines.

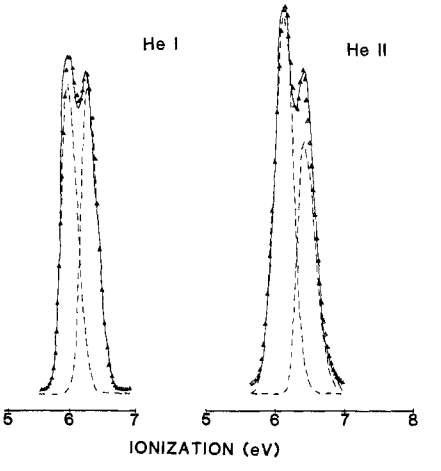

Figure 12. Photoelectron spectra of **2a** in the onset region, comparing results with He I and He II photon energies.

In Figure 11 are shown He I spectra of the cofacial dimer **2a**. It can be seen that the onset band now appears as a doublet

(components a and a') with a splitting of 0.29 ± 0.03 eV. This splitting is a measure of the HOMO–HOMO interaction energy, $2t$ (cf. Figure 1). In comparison to the energy of band a in **3a**, the center-of-gravity of the a,a' doublet is shifted 0.20 (3) eV to lower energy, indicating greater stabilization of the radical cation state in the dimer. Figure 12 shows the change in the onset ionization region of **2a** as a function of photon energy. Clear changes in cross section are observed on going from He I to He II. Further interpretation is reserved for the following section.

Electronic Structure Studies. The simplest electronic structure model for understanding electronic charge transport in linear chain or polymeric conductors is the one-dimensional tight-binding band.[1,7,8] In this model, which is simply the Hückel model with the molecular HOMO's used in place of the carbon π as the local basis functions, only two energy terms are retained in the electronic Hamiltonian. The first of these is the single-site electron energy (corresponding to the binding energy of the electron in the HOMO), and the second is the nearest-neighbor electronic tunneling matrix element, usually denoted t, which is the analogue of the Hückel β integral. Overlap integrals among the HOMO's on the monomeric subunits are neglected in this model. The splitting of monomer HOMO's upon forming a dimer is $2t$ and the bandwidth is $4t$ (Figure 1). While this tight-binding, narrow-band picture seems reasonable and is generally well accepted for the description of the conductivity in linear chain conductors and conductive polymers, still the details of the conduction mechanism, as well as the numerical values of the bandwidth and the electron/vibration and electron/libration coupling constants, are not known a *priori*. The dimers studied here provide a straightforward system for application of molecular subunit calculations to understand the conductive behavior, since predicted values from the theoretical calculations may be compared both with observations on the species (monomer and dimer) actually studied and with macroscopic polymeric samples. Our calculations, then, are aimed both at interpretation of the spectra and electronic structures of $Si(Pc)(OR)_2$ and ROSi(Pc)OSi(Pc)OR compounds (**3a**, **2a**) and at computing and interpreting the energy splitting of the highest occupied orbitals which, in the tight-binding model of Figure 1, is half the bandwidth.

Another role of these calculations is to help disentangle the "bare" bandwidth, as determined from the dimer splitting at frozen geometry, from a possible-narrowed bandwidth, which might occur due to electron/vibration coupling in the chain. Such a reduction of the bandwidth by vibronic coupling, which has been invoked in several linear chain discussions,[53] would be analogous to Huang–Rhys factors in color center spectra, to Ham reduction factors in Jahn–Teller systems, to Franck–Condon factors in optical spectra, or to Debye–Waller factors in scattering. It would produce an effective bandwidth which would be smaller than the value $4t$ (deduced from the tight-binding model of Figure 1) because of vibrational overlap factors.

Computational Details. The DVM-Xα technique is discussed extensively elsewhere.[14-17] It is a first-principles method, with no adjustable parameters. It involves use of a basis set expansion of the wave function for the molecule as a linear combination of atom-centered numerical basis functions. The numerical feature is particularly important, since the ring–ring interactions that are responsible for the bandwidth occur at a distance of 3.33 in iodine-doped $[Si(Pc)O]_n$; this is in the tail region of the usual valence orbitals and is therefore described quite poorly by the usual molecular Gaussian- or Slater-type basis orbitals. The linear combination coefficients are the eigenfunction unknowns and are determined by solution of the one-electron local density equation (eq 2). Here P_i and x_i are momentum and coordinate of the i^{th}

$$\{P_i^2/2m_e + V_{Coul}(x_i) + V_{xc}(x_i) - \epsilon_i\}\psi_i(x_i) = 0 \qquad (2)$$

electron, which is in MO $\psi_i(x_i)$ with energy ϵ_i. The Coulomb potential $V_{Coul}(x_i)$ includes the electron–nucleus attraction as well as the electron–electron repulsion, while the exchange/corelation term $V_{xc}(x_i)$ is a local functional of the electron density $\rho(x)$. Since V_{Coul} and V_{xc} depend on ρ, which in turn depends on x, eq must be solved self-consistently to obtain final values for ψ and ϵ.

For the present calculations, a potential fit including[14] terms of angular momentum $l = 0$ and 1 on N, C, and O and $l = 0$, 1, and 2 on Si was used. The basis set in which ψ is expanded was chosen in two different ways. The smaller valence basis included 1s on H, 1s,2s,2p, on C, N, and O, and 1s,2s,2p,3s,3p,3d on Si. For the extended basis 3s and 3p functions were added on N and C, while 4s and 4p were added on Si. The inclusion of such functions should be quite helpful in attaining quantitative accuracy in the calculations, especially in the excited states.

The exchange/correlation potential was chosen in two different ways. For most of our work, the simple Slater form (eq 3)[54] was

$$V_{xc}(\vec{x}) = -3\alpha[3\rho(\vec{x})/8\pi]^{1/3} \qquad (3)$$

chosen, with exchange parameter α chosen as 0.70. For some calculations, the Hedin–Lundqvist[55] exchange/correlation potential, which involves a more accurate and elaborate form based on results for the electron gas, was used. All calculations were carried to full self-consistency (energies ϵ_i converged to at least 0.002 eV).

The $Si(Pc)(OH)_2$ Monomer. Calculations were carried out by using two different basis sets (valence and extended) with two different choices for the exchange/correlation functions (simple Slater and Hedin–Lundqvist). All electrons were included. For the monomer we chose a planar phthalocyanine ring with the metrical parameters of $Si(Pc)[OSi(CH_3)_3]_2$;[26b] the H–O–Si angle was 180° and the O–H and Si–O bond lengths were 0.957[56] and 1.636 Å, respectively. Two sorts of calculations were performed: closed-shell, ground-state studies to examine the orbital energy levels and transition-state work to find optical transition energies and ionization energies.

Figure 13 shows the energy level diagrams obtained by using the extended basis set with d orbitals on Si and supplementary functions on Si, N, and C. While this basis reproduces the energy

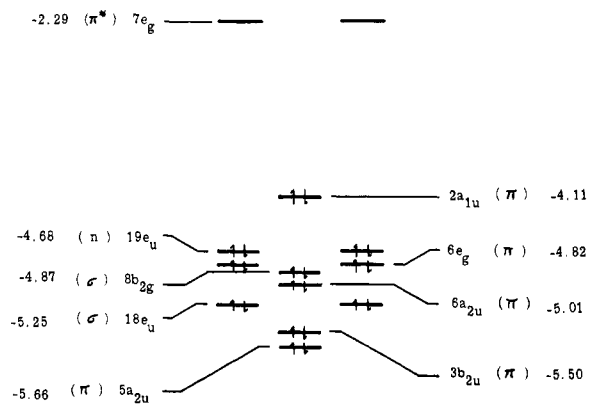

Figure 13. Energy levels for the valence orbitals of $Si(Pc)(OH)_2$ derived from DV-Xα calculations with an extended basis set. Units are in electron volts. To obtain ionization potentials, these numbers are corrected for relaxation effects to obtain the data in Table X.

(53) See, for example: (a) Chaikin, P. M.; Garito, A. F.; Heeger, A. G. *J. Chem. Phys.* **1973**, *58*, 533–534. (b) Bright, A. A.; Chaikin, P. M.; McGhie, A. R. *Phys. Rev. B: Solid State* **1974**, *10*, 3560–3568.

(54) Slater, J. C. "Quantum Theory of Molecules and Solids"; McGraw-Hill: New York, 1974; Vol. 4.

(55) Hedin, L.; Lundqvist, B. I. *Solid State Phys.* **1969**, *23*.

(56) Typical value based on known compunds containing OH bonded to electropositive centers: Landolt-Bernstein, V. T. "*Structure Data of Free Polyatomic Models*"; Springer Verlag: Berlin, 1976 and references therein.

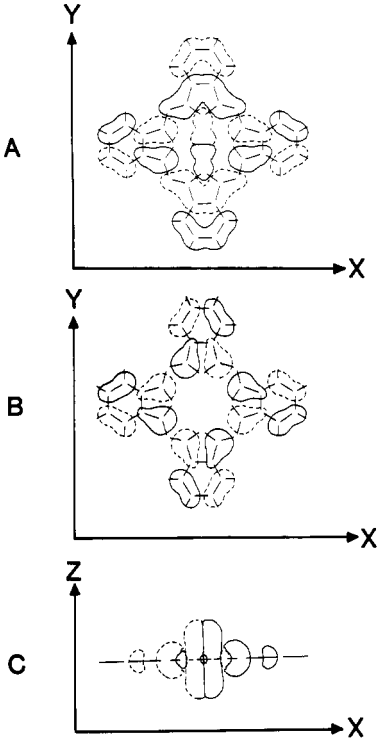

Figure 14. Graphic representations of the following molecular orbitals of $Si(Pc)(OH)_2$ in order of decreasing energy: A, $7e_g$ (LUMO) viewed perpendicular to the ring plane; B, $2a_{1u}$ (HOMO) viewed perpendicular to the ring plane; C, $19e_u$ viewed parallel to the ring plane.

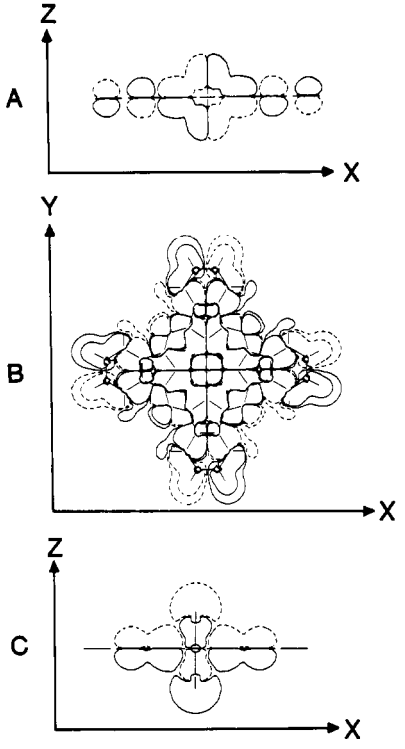

Figure 15. Graphic representations of the following $Si(Pc)(OH)_2$ molecular orbitals (in order of decreasing energy): A, $6e_g$ viewed parallel to the ring plane; B, $8b_{2g}$ viewed perpendicular to the ring plane; C, $6a_{2u}$ viewed perpendicular to the ring plane.

ordering seen in other calculations,[33a,34,35a,b] the minimum basis set inverts the two highest occupied orbitals. When the extended basis is used, the ordering of the π levels and their separations also agree well with semiempirical (PPP) calculations.[33a] In Figures 14 and 15 are shown contour diagrams for some of the important molecular orbitals. The $7e_g$ LUMO (Figure 14A) is heavily π-bonding within the phthalocyanine ring as well as silicon-oxygen π-bonding. The $2a_{1u}$ HOMO (Figure 14B) is composed entirely of out-of-plane carbon p_z functions localized predominantly on C_a (see structure B). This MO has no amplitude on silicon or oxygen, arguing that the siloxane backbone plays no significant role in the $[Si(Pc)O]_n$ charge-transport process (i.e., it is not part of the band structure). The degenerate $19e_u$ MO (Figure 14C) is primarily silicon–oxygen p–p π–bonding. It is also weakly σ-bonding to the isoindoline rings. Slightly lower in energy is the $6e_g$ orbital (Figure 15A) that is composed chiefly of oxygen lone pairs. As can be seen in the figure, these lone pairs are involved in some π-bonding with the phthalocyanine macrocycle. The form of the $19e_u$ and $6e_g$ orbitals is somewhat reminiscent of the pattern in linear dioxo cations.[57] It is possible that such interactions may influence the conformational preferences of various axial rotamers and stabilize the obtuse Si–O–R angles seen. The $8b_{2g}$ MO (Figure 15B) is largely C–C and C–H σ-bonding. It is also slightly C_aN_m (structure B) σ-bonding in character but has nodal planes passing through N_p atoms. Still lower in energy is the $6a_{2u}$ MO (Figure 15C) which is primarily silicon–oxygen and silicon–hydrogen σ-bonding as well as π-bonding within the macrocyclic ring.

Table XI. Calculated Optical and Ionization Energies for $Si(Pc)(OH)_2$

	calcd	obsd[d]
Ionization Energy, eV		
$2a_{1u}$	6.8[a]	6.46
$2a_{1u}$	5.6[b]	6.46
$2a_{1u}$	9.3[c]	6.46
Optical Excitations, nm		
$2a_{1u} \rightarrow 7e_g$ ($\pi \rightarrow \pi^*$)	672.5	671
$6a_{2u} \rightarrow 7e_g$ ($\pi \rightarrow \pi^*$)	443.3	445
$19e_u \rightarrow 7e_g$ ($n \rightarrow \pi^*$)	442.5	
$3b_{2u} \rightarrow 7e_g$ ($\pi \rightarrow \pi^*$)	373	340
$5a_{2u} \rightarrow 7e_g$ ($\pi \rightarrow \pi^*$)	351	

[a] Extended basis, Hedin–Lundqvist potential. [b] Extended basis, Slater potential. [c] Valence basis, Slater potential. [d] Data for compound **3a**.

The assignment of the PES spectra follows from the DV-Xα results (Tables X and XI). The $Si(Pc)(OH)_2$ transition-state ionization potential (from the HOMO), calculated with the extended basis set and Hedin–Lundqvist potential (6.8 eV) is in favorable agreement with the experimental band a (Figure 9) ionization energy for **3a** of 6.46 eV. This is especially true since the capping groups may have the effect of slightly lowering the ionization potential. The band a in Figure 9 is thus assigned to ionization from the $2a_{1u}$ HOMO. The associated vibrational interval of 1240 ± 200 cm^{-1} (Figure 10) is reasonably associated with an Si(Pc) skeletal mode[10,27] and agrees well with the π-bonding character of the HOMO. In regard to assigning the other PES features, transition-state energies have not been computed for the other MO's. Since Koopman's theorem is not valid for Xα calculations, the ionization potentials should be calculated by using Slater's transition-state procedure,[54] which corrects the calculated orbital energies for relaxation effects. Differential relaxation effects (relative to ligand-based MO's) should only be important for orbitals having significant metal d orbital amplitudes.[58] Thus, for the present system, the sequence of transition-state energies and corresponding ground-state eigenvalues are expected to be very similar. As can be seen from the assignments in Table X, the DV-Xα eigenvalues provide a very accurate fitting of the experimental ionization energies when they are rescaled in order to fit the ionization energies of the first two PES bands. This rescaling has the same effect as would transition-state calculations and permits the eigenvalues (Figure 13) to be converted to ionization energies (Table X) without the

(57) Fragala, I.; Condorelli, G.; Tondello, E.; Cassol, A. *Inorg. Chem.* **1979**, *17*, 1375 and references therein.
(58) See, for example: Veillard, A.; Demuynck, J. In "Modern Theoretical Chemistry"; Schaefer, H. F., Ed.; Plenum Press: New York, 1977; Vol. 4, pp 187–222.

Table XII. Dimer Splittings and Experimental Conduction Bandwidths for $[Si(Pc)O]_n$

method	bandwidth, eV	ref
DVM calculation[a] (bandwidth = twice dimer splitting)	0.76	this work
photoemission[a]	0.58 (6)	this work
Drude analysis[b]	0.60 (6)	10a
susceptibility[b]	0.32 (3)	10a

[a] Result for dimer **2a**. [b] Result for $\{[Si(Pc)O]I_{1.12}\}_n$.

necessity of doing transition-state calculations for each ionization. Within the context of the present assignment, it is worth noting that the relative intensities of bands b–e in **3a** do not rigorously reflect the occupancy ratios of the corresponding MO's. Some of this discrepancy is no doubt due to underlying ionizations due to MO's centered on the $-Si[C(CH_3)_3](CH_3)_2$ capping groups, which are expected[59] to have ionizations in the b–e spectral region.

The observed and calculated $Si(Pc)(OH)_2$ optical transitions are given in Table XI. The agreement is generally quite good; as has been pointed out previously,[33,34] the first few optical transitions in phthalocyanines do not involve extensive configuration mixing, so that straightforward single configuration pictures describe the transitions well. It is, however, necessary to use the extended basis set to describe these fairly energetic transitions, since the valence basis is matched to the atoms in the ground-state molecule and really cannot be expected to describe very well an excitation with 15 000 cm^{-1} or more of energy. The high accuracy of these transition-state calculations strengthens the earlier assignments of the Q band near 670 nm as due to $a_{1u} \rightarrow e_g$ ($\pi \rightarrow \pi^*$) and the Soret-type bands near 340 nm as due to $a_{2u} \rightarrow e_g$ ($\pi \rightarrow \pi^*$) and $b_{2u} \rightarrow e_g$ ($\pi \rightarrow \pi^*$), respectively. The earlier suggestion[34] that the 340-nm band is broadened due to $n \rightarrow \pi^*$ excitaions is not borne out by our calculations, since the intensity of these excitations is quite small. The $3b_{2u} \rightarrow 7e_g$ transition, which has not so far been discussed in connection with the breadth of the 340-nm band, might make some contribution. The calculation of the $6a_{2u} \rightarrow 7e_g$ transition using the extended basis predicts an excitation of 443.3 nm, compared to 445 nm from experiment. Curiously, however, this band is considerably less intense (Figure 5) than might a priori be expected. Indeed, an approximate transition moment calculation also predicts a higher oscillator strength than observed. The small peaks near 600 and 650 nm are probably due to vibronic effects.

The HOSi(Pc)OSi(Pc)OH Dimer Orbital Splittings and Bandwidth. While $K_2Pt(CN)_4Br_{0.3}$ and the other metal chain salts conduct by means of a band built of d_{z^2} orbitals, there is considerable reason to think that for the polymeric phthalocyanines, as well as the stacked metallomacrocyclic conductors such as $H_2(Pc)I$, NiPcI, and planar organic conductors such as TTF–TCNQ or $(TTT)_2I_3$, the conduction occurs through overlapping π orbitals on the carbon atoms or heteroatoms in the plane. In the Pc systems, these reasons include the expected weakness of the oxygen-bridged metal overlaps, the similarity of the conductive behavior of the $H_2(Pc)I$,[10c,60] Ni(Pc)I,[9,10,45] and doped $[Si(Pc)O]_n$[9,10] materials, EPR data,[9,10,60] and the rather similar photoemission spectra of various metallophthalocyanines.[24]

The DV-Xα code with self-consistent multipolar potentials is particularly appropriate to describe π-π interactions in cofacial metallomacrocyclic dimers **2** and the spectroscopic manifestations thereof. These are one-electron properties, for which Xα methods are very well-suited, and the inclusion of relaxation effects using the transition state should allow optical spectroscopic and PES properties to be handled especially well. The use of an extensive numerical basis set, as employed in our DVM work, is quite important for finding accurate splittings, which are dominated by interactions among π orbitals quite far out into their tail regions; in this region, the usual analytic basis functions may be inaccurate (vide supra).

DVM calculations were undertaken on the cofacial dimer HOSi(Pc)OSi(Pc)OH, assuming the OSi(Pc)OSi(Pc)O core structural parameters of **2a** in Table VIII and linear SiOH functionalities (O–H distance = 0.957 Å). Because of the size of the molecule, only a limited valence orbital basis set calculation could be carried out. The valence basis was orthogonalized against the "frozen core" atomic orbitals. The most interesting result is that the calculated splitting ($2t$) between the two highest occupied dimer molecular orbitals is 0.38 eV. This would imply a tight-binding bandwidth, without polaron narrowing, of $4t = 0.76$ eV, which compares extermely well with the experimental values compiled in Table XII, including the value of $2t = 0.29 \pm 0.03$ eV deduced from the aforementioned photoelectron spectrum of **2a** (Figures 11 and 12). These comparisons, coupled with the fact that no pronounced vibronic sidebands are observed in the photoemission spectrum (such sidebands would arise if there were a major geometry change upon electron transfer), show convicingly that there are no important polaronic band-narrowing effects in these polymers and that the tight-binding matrix element t gives the splitting $2t$ and the bandwidth $4t$ quite accurately. (There are changes in the splittings as the molecules vibrate or librate with respect to one another, and these acutally determine the conductivity of the chain. Their study using DVM methods will be reported elsewhere.)

In regard to details of the PES spectra, it is of interest to note that the roughly 1:1 intensity ratio of band a:a′ in the He I spectrum of **2a** shifts to ca. 1.5:1 in the He II spectrum (Figure 12). Because the more intense band a results from ionizing an MO of a_2 symmetry that cannot mix with silicon 3d atomic orbitals, it is suggested that the changes in relative a:a′ intensity must reflect differences in spatial localization[61] of the symmetric and antisymmetric MO combinations being ionized.

The Si(Pc) orbitals that give rise to the splitting are of pure carbon π-type—they are the $2a_{1u}$ species of the monomer and have a nodal plane in the plane of the macrocycle, with two more nodal planes passing through the coordinating nitrogens. Thus these $[M(Pc)O]_n$ conducting polymers, like the TTF and TCNQ and Pc stacked conductors, are expected to show a mobility mechanism largely involving the p–π orbitals on carbon. The present dimer calculations, used to find the bandwidth, were performed only in the valence basis. While this is satisfactory for the ground-state properties, we see from the monomer results that the extended basis is needed for accurate representation of excited states.

Conclusions

This work demonstrates that correlated experimental and theoretical studies on isolable, monomeric, and dimeric stack fragments can provide valuable information on the electronic structure of "molecular metals". In particular, both ex situ spectroscopic measurments and first-principles local exchange DV-Xα calculations on dimer fragments can provide accurate, quantitative descriptions of π–π interactions and tight-binding bandwidths in the actual low-dimensional solid-state molecular arrays. In the case of cofacially arrayed metallomacrocyclic conductors, a better insight into the conduction pathways, the importance of polaronic band narrowing effects, the relative accuracy of various in situ assessments of bandwidth (e.g., magnetic susceptibility, optical reflectivity), and those parameters critical to the design of new molecular and macromolecular "metals" is provided.

Acknowledgment. This research was supported by the NSF through the Northwestern Materials Research Center (Grant DMR82-16972), by the Office of Naval Research (to T.J.M), by the U.S.–Israel Binational Science Foundation (to F.H.H. and

(59) Evans, S.; Green, J. C.; Jackson, S. E. *J. Chem. Soc. Faraday Trans. 2* **1973**, *69*, 191–195.

(60) (a) Lyding, J. W.; Inabe, T.; Burton, R. L.; Kannewurf, C. R.; Marks, T. J. *Bull. Am. Phys. Soc.* **1984**, *29*, KH3. (b) Inabe, T.; Lyding, J. W.; Burton, R. L.; Kannewurf, C. R.; Marks, T. J. *Mol. Cryst. Liq. Cryst.*, in press.

(61) Price, W. C.; Potts, A. W.; Streets, G. D. In "Electron Spectroscopy"; Shirley D. A. Ed.; North-Holland: Amsterdam, 1972; pp 187–198.

T.J.M), by the Chemistry Division of NSF (M.R.), and by the NATO Research Grants Program (Grant 068/84 to I.F. and T.J.M.). I.F. thanks the Fulbright Foundation for a travel grant. We thank Professor Martin Gouterman for several helpful suggestions.

Supplementary Material Available: A table of anisotropic temperature factors (Table VII) and a listing of observed and calculated structure factors from the final cycle of least-squares refinement (13 pages). Ordering information is given on any current masthead page.

Infrared Laser Photochemistry of SiH_4–HCl Mixtures[1]

C. B. Moore, J. Biedrzycki,† and F. W. Lampe*

Contribution from the Davey Laboratory, Department of Chemistry, The Pennsylvania State University, University Park, Pennsylvania 16802. *Received May 25, 1984*

Abstract: The infrared laser photochemistry of SiH_4–HCl mixtures has been studied in a pressure range of 28–60 torr and in a temperature range of 295–414 K. The gaseous products observed are H_2, Si_2H_6, SiH_3Cl, SiH_2Cl_2, and $SiHCl_3$ with trace amounts of Si_3H_8 and Si_2H_5Cl. As is usual in silane decompositions, a solid product containing silicon, hydrogen, and perhaps very small amounts of chlorine was also formed. The photochemical conversion is best described by initial decomposition of SiH_4 to SiH_2 and H_2 followed by competition of SiH_4 and HCl for SiH_2 molecules. The simultaneous formation of all chlorosilanes suggests that decomposition of the initial product of SiH_2–HCl reaction leads in turn to SiHCl and $SiCl_2$ molecules. Studies of the temperature dependence of the rates of the competing reactions indicate that the activation energy for insertion of SiH_2 into HCl is less than 1.3 kcal/mol.

Recent studies of the infrared laser induced decomposition of pure SiH_4,[2,3] SiH_4–SiF_4[4] mixtures, and SiH_4–PH_3[5] mixtures have shown that the predominant primary photodecomposition is to SiH_2 and H_2, paralleling what is thought to be the mechanism of the purely thermal homogeneous decomposition of SiH_4. It therefore appears that the infrared laser induced decomposition of SiH_4 would be a good source of SiH_2 for study of the interaction of these reactive molecules with other substrates.

It is known that SiH_2 will insert readily into Si–H bonds.[2,4,6–12] Moreover, there is evidence that silylenes insert into the O–H bonds of alcohols[10] and into Si–Cl bonds in halosilanes.[11,12] The insertion of SiH_2 into the strong H–H bond of molecular hydrogen has been reported,[13] and it is of interest to inquire if SiH_2 will insert into an equally strong bond involving hydrogen that resides in an equally simple molecule. Hence, we have conducted a study of the infrared laser photochemistry of SiH_4–HCl mixtures. This paper is a report of our results.

Experimental Section

The infrared laser photodecompositions were carried out in a cylindrical stainless-steel cell having a diameter of 3.45 cm and a length of 15.5 cm. A pinhole leak, located in the wall of the photolysis cell, led directly into the ionization source of a time-of-flight mass spectrometer. The ends of the photolysis cell were fitted with NaCl windows sealed in place by O-ring supports. The cell was mounted so that the laser beam was perpendicular to the axis of the time-of-flight mass spectrometer. Molecules leaving the cell, along the axis of the flight tube of the mass spectrometer, reach the ionization source after a transit time of, at most, 2–3 ms.

The source of infrared radiation was a CO_2 TEA laser (Lumonics Research Ltd., Model 103-2) pulsed at a frequency of 0.5 Hz. All irradiations were carried out with an unfocussed beam and with the laser turned to the P(20) line of the 10.6 μm band, i.e., at 944.19 cm^{-1}; this corresponds to a photon energy of 0.11706 eV. The average cross section of the beam was 5.94 cm^2, and the incident energy, as measured by a GenTec joulemeter and an evacuated photolysis cell, was 4.17 J/pulse, resulting in an incident fluence of 0.70 J/cm^2. The laser beam illuminated approximately 64% of the photolysis cell volume.

During a photolysis the concentrations of SiH_4, HCl, H_2, Si_2H_6, SiH_3Cl, SiH_2Cl_2, and $SiHCl_3$ were determined mass spectrometrically by measurement of the intensities of the ions at m/z 31, 36, 2, 62, 64, 99, and 133, respectively, which are generated in the ion source of the mass spectrometer. Calibrations for quantitative measurements at the above masses, in which ion currents are related to molecular concentrations, were carried out by using pure samples of SiH_4, HCl, H_2, Si_2H_6, SiH_2Cl_2, and $SiHCl_3$. A pure sample of SiH_3Cl was not available, and so the initial rates of formation of this substance were calculated by the material balance in (1). This assumes, of course, that all of the chlorine atoms

$$\left(\frac{d[SiH_3Cl]}{dt}\right)_0 = -\left[\left(\frac{d[HCl]}{dt}\right)_0 + 2\left(\frac{d[SiH_2Cl_2]}{dt}\right)_0 + 3\left(\frac{d[SiHCl_3]}{dt}\right)_0\right] \quad (1)$$

from the reacted HCl remain in the gas phase as SiH_3Cl, SiH_2Cl_2, and $SiHCl_3$. Using a reported mass spectrum[14] and estimates of the ionization cross section of SiH_3Cl from interpolation of cross sections for SiH_4, SiH_2Cl_2, $SiHCl_3$, and $SiCl_4$, it is clear that the preponderance of the Cl in the reacted HCl appears as SiH_3Cl and that the initial rate of SiH_3Cl formation determined by (1) is not in serious error, certainly not more than 15%.

SiH_4 was obtained from the Matheson Co. and further purified by vacuum distillation. Si_2H_6 was synthesized by using methods described previously[15] and was also purchased from Merck and Co. SiH_2Cl_2 was obtained from Petrarch Systems, and $SiHCl_3$ was purchased from Alfa

† Present address: Institute of Chemistry, University of Gdansk, Gdansk, Poland.

(1) U. S. Department of Energy Document No. DE-AS02-76ER03416-32.
(2) Longeway, P. A.; Lampe, F. W. *J. Am. Chem. Soc.* **1981**, *103*, 6813.
(3) O'Keefe, J. F.; Lampe, F. W. *Appl. Phys. Lett.*, in press.
(4) Longeway, P. A.; Lampe, F. W. *J. Phys. Chem.* **1983**, *87*, 354.
(5) Blazejowski, J.; Lampe, F. W., *J. Photochem.* **1982**, *20*, 9.
(6) Purnell, J. H.; Walsh, R. *Proc. R. Soc. London, Ser. A* **1966**, *293*, 543.
(7) Newman, C. G.; O'Neal, H. E.; Ring, M. A.; Leska, F.; Shipley, N. *Int. J. Chem. Kinet.* **1979**, *11*, 1167.
(8) Neudorfl, P.; Jodhan, A.; Strausz, O. P. *J. Phys. Chem.* **1980**, *84*, 338.
(9) Cochet, G.; Mellottee, H.; Delbourgo, R. *J. Chim. Phys.* **1974**, *71*, 1363.
(10) Atwell, W. H. U.S. Patent 3 478 078, Nov 1969.
(11) Timms, P. L. *Inorg. Chem.* **1968**, *7*, 387.
(12) Gaspar, P. P.; Herold, B. J. *In* "Carbene Chemistry", 2nd ed.; Kirmse, W., Ed.; Academic Press: New York, 1971; p 504.
(13) John, P.; Purnell, J. H. *J. Chem. Soc., Faraday, Trans. 1*, **1973**, *69*, 1455.
(14) Potzinger, P., private communication 1982.
(15) Perkins, G. G. A.; Lampe, F. W. *J. Am. Chem. Soc.* **1980**, *102*, 3764.

0002-7863/84/1506-7761$01.50/0